Bayesian Population Pharmacokinetic/Pharmacodynamic Modeling to Study the Effect on the Cardiovascular Syndrome of the QTc Interval Prolongation of Non-antiarrhythmic Drugs

Giovanni Smania

July 15, 2013

Alla mia intera famiglia,
fonte inesauribile di motivazione e supporto.

Contents

Abstract

Assessment of the propensity of non-antiarrhythmic drugs in prolonging QT/QTc interval is critical for the progression of compounds into clinical development. Given the similarities in QTc response between dogs and humans, dogs are often used in pre-clinical cardiovascular safety studies. The current regulatory guidelines are based on simple statistical analyses of QT data, thereby ignoring any potential exposure-effect relationship and nonlinearity in the underlying physiological fluctuation in QT values. The objective of this analysis is to adopt a model based approach to assess the QT-prolonging effects in dogs and humans of GSK945237, a new compound under development. Pharmacokinetic and pharmacodynamic data from experiments in conscious dogs and clinical trials following administration of GSK945237 were used. First, pharmacokinetic modelling was applied to derive drug concentrations at the time of each QT measurement. A Bayesian PKPD model was then used to describe QT prolongation, which allows discrimination of drug-specific effects from other physiological factors known to alter QT interval duration. Results from this analysis show the drug under investigation is not prone to cause hazardous increases in the QT interval for both humans and dogs. Further, the PKPD model is capable to predict both preclinical and clincal data, suggesting it might be used for future translational research in the field of QT prolongation.

Chapter 1

Introduction

1.1 Physiolgy of the QT Interval and the Drug Effect on it

The QT interval is the portion of the Electrocardiographic signal (ECG) in between the beginning of the QRS complex and the end of the T-wave (Figure 1.1). It represents the time between the onset of electrical depolarization of the ventricles and the end of their repolarization, that is, it reflects the duration of individual action potentials in the cardiac myocytes.
QT interval is affected by several sources of variability of diverse nature. As one would excpect, the QT interval duration is strictly related to the RR interval (i.e. the cardiac period). In fact it is well known that in order to improve the detections of threatening QT prolongations, the measured QT has to be corrected for changes in RR interval, taking the name of *corrected* QT interval (QTc). Other subject-related factors potentially affecting the QT/QTc interval are:

1. Genetic (long QT syndrome)
2. Food intake
3. Circadian rhythm
4. Sex
5. Obesity
6. Physical activity
7. Blood glucose level
8. Blood pressure
9. Age

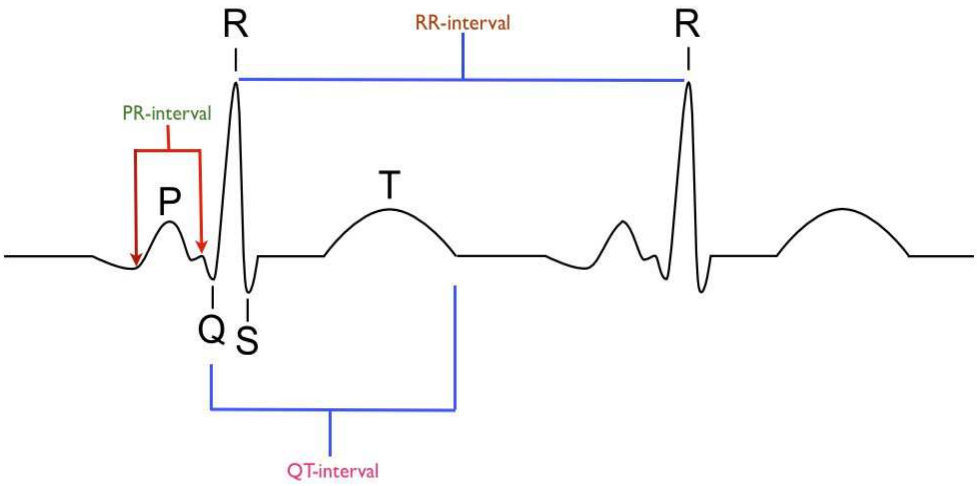

Figure 1.1: Schematic ECG trace showing the different waves and intervals that characterize it.

In cardiovascular safety assessment studies, considerable attention has been paid due to the fact that both antyarrhythmic and non-antyarrhythmic drugs may prolong the QT interval.
QT prolonging compounds do that by blocking the so-called human *Ether-á-go-go* Related Gene (hERG), a gene coding for the alpha subunit of a potassium ion channel (also called, with a bit of ambiguity, hERG) which modulates the repolarizing current I_{Kr} in the cardiac action potential.
A possibile explanation for such drug effect has been given by Milnes et al. [1]. Starting from the hypothesis that the high-affinity drug-binding sites are within the vestibule of the channel, they state that the absence of highly conserved prolines (normally present in K^+ channels) at hERG ammino-acid positions may suggest that a "kink" is absent, thereby more space is available within the vestibule. A potential effect of this increasing in space inside the vestibule of the hERG would be the ability of a wide variety of drugs to gain access to binding sites inside the pore.
The blockade of hERG channel implies a lower conductivity of K^+ ions (i.e. a lower I_{Kr}), whom reflects on a bigger duration of the action potential of cardiac myocytes, ending with a slower ventricular repolarization and a longer QT interval (Figure 1.2).

1.2 Motivation

Non clinical and clinical cardiovascular toxicities are one of the main safety reasons for

(i) drug discontinuation throughout all stages of drug discovery and development;

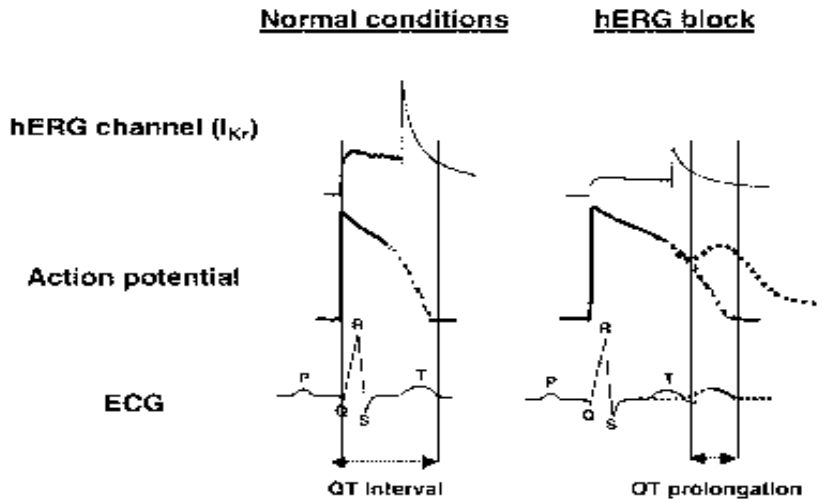

Figure 1.2: hERG blockade proccess.

(ii) serious adverse events and adverse drug reactions during clinical development and

(iii) post marketing drug withdrawal.

Among those, prolongation of the QT/QTc interval had been the reason for one-third of all drug withdrawals for the period 1990-2006 [2].
Although drug-induced lengthening of the QT/QTc interval is not a safety concern in itself, this effect has been associated with the occurrence of a rare, life-threatening ventricular tachycardia named *Torsades de Pointes* (TdP) [3]. Therefore the ability to assess QT/QTc prolongation effects as early as possible during the course of the clinical development of a new compound is helpful not only in understanding the potential risk-benefit ratio of the molecule but also in deciding whether to progress with the development of the drug, thereby avoiding unnecessary costs.
According to the most current regulatory guideline - the International Conference of Harmonisation (ICH) E14 Document [4] - the critical threshold for cardiovascular safety concerns in the QTc-interval increasing is equal to 10 msec. Therefore, in the context of QTc prolongation, the application of translational methods makes possible the prediction of QTc lenghtening in humans starting from outcomes obtainend in preclinical studies; with regard to this, the work that has been proposed provides a tool to investigate such translation and to identify the gap between preclinical and clinical findings. Further, given that the protocol suggested by the ICH E14 can lead to biased results for several reasons [5], in order to increase the reliability of potential conclusions the QT interval has been described by means of nonlinear mixed-effects modeling techniques applied in a bayesian framework. Non linear mixed-effect modeling helps to overcome issuses due to managing sparse data

coming from different individuals (which is the case for QT measurements in humans), while a bayesian approach fits naturally into decision analysis since it allows to obtain the full posterior probability plus the credible intervals of a parameter of interest instead of a puntual estimate with its confidence interval. These two aspects will be treated widely later (see 1.3 and 1.4).

1.3 Basics of Non Linear Mixed Effect Methods

Non Linear Mixed Effect (NLME) models, also called hirerchical models, are used in population analysis related fields such as environmental health, agriculture and pharmacokinetics/pharmacodynamics.
Population analysis is an alternative method to individual analysis that has its strength in extrapolating information from sparse data coming from different individuals, assuming that each individual feature comes from a distribution of that feature which is representative of the entire population of interest.
The mathematical formulation of the model will be presented (1.3.1), followed by an applied pharmacokinetic example (1.3.2).

1.3.1 The Basic Model

NLME modelling is more complex than standard modelling techniques, and has to be stratified into two hirerchical steps.

1. *Stage 1: Individual-Level model*

   The individual step aims to define the measure model:

   - $z_{i,j}$: the j^{th} measure ($j = 1, ..., N$) for the i^{th} subject ($i = 1, ..., K$), collected at time $t_{i,j}$
   - $\mathbf{u}_i$: vector of additional conditions under which subject i is observed
   - $\mathbf{p}_i$: vector of model parameters specific to subject i ($M \times 1$)
   - $f(t_{i,j}, \mathbf{u}_i, \mathbf{p}_i)$: non-linear relationship between $z_{i,j}$ and $(t_{i,j}, \mathbf{u}_i, \mathbf{p}_i)$
   - $\epsilon_{i,j}$: random error due to uncertainty in the measure denoting within-individual variabilty

   If we consider an additive residual error, the individual model can be written as

$$z_{i,j} = f(t_{i,j}, \mathbf{u}_i, \mathbf{p}_i) + \epsilon_{i,j}. \tag{1.1}$$

Defining

$$\mathbf{z}_i = \begin{bmatrix} z_{i,1} \\ z_{i,2} \\ \vdots \\ z_{i,N} \end{bmatrix} \mathbf{f}_i(\mathbf{p}_i) = \begin{bmatrix} f(t_{i,1}, \mathbf{u}_i, \mathbf{p}_i) \\ f(t_{i,2}, \mathbf{u}_i, \mathbf{p}_i) \\ \vdots \\ f(t_{i,N}, \mathbf{u}_i, \mathbf{p}_i) \end{bmatrix} \boldsymbol{\epsilon}_i = \begin{bmatrix} \epsilon_{i,1} \\ \epsilon_{i,2} \\ \vdots \\ \epsilon_{i,N} \end{bmatrix}$$

it is possible to summurize equation (1.1) as

$$\mathbf{z}_i = \mathbf{f}_i(\mathbf{p}_i) + \boldsymbol{\epsilon}_i \tag{1.2}$$

where a classical assumption on $\boldsymbol{\epsilon}_i$ is

$$\boldsymbol{\epsilon}_i | \mathbf{p}_i \sim \mathcal{MVN}(0, \mathbf{R}_i(\mathbf{p}_i, \boldsymbol{\xi}))$$

with $\boldsymbol{\xi}$ costant accros individuals. For example it might need to incorporate a proportional error model, therefore $\boldsymbol{\xi}$ will be constant ($= \sigma^2$) and $\mathbf{R}_i$ will be

$$\mathbf{R}_i = \sigma^2 \mathbf{f}_i(\mathbf{p}_i) = \sigma^2 \begin{bmatrix} f(t_{i,1}, \mathbf{u}_i, \mathbf{p}_i) & 0 & \cdots & 0 \\ 0 & f(t_{i,2}, \mathbf{u}_i, \mathbf{p}_i) & \cdots & 0 \\ \vdots & \vdots & \ddots & \vdots \\ 0 & 0 & \cdots & f(t_{i,N}, \mathbf{u}_i, \mathbf{p}_i) \end{bmatrix}$$

2. *Stage 2: Population-Level model*

To account for inter-individual variation of parameters $\mathbf{p}_i$ among individuals, a model for $\mathbf{p}_i$ has to be specified. The population step provides this model:

- $\mathbf{a}_i$: vector of characteristics of subject i (named covariates)
- $\boldsymbol{\eta}_i$: vector of random effects for subject i conveying inter-individual variation
- $\boldsymbol{\theta}$: vector of fixed effects expressing features common to the entire population
- $\mathbf{d}$: M-dimensional vector function

Then a general model for $\mathbf{p}_i$ is given by

$$\mathbf{p}_i = \mathbf{d}(\mathbf{a}_i, \boldsymbol{\eta}_i, \boldsymbol{\theta})$$

where a classical assumption on $\boldsymbol{\eta}_i$ is

$$\boldsymbol{\eta}_i \sim \mathcal{MVN}(0, \boldsymbol{\Omega}) \tag{1.3}$$

1.3.2 Pharmacokinetic Application of a NLME Model

Pharmacokinetics is the study of the time course of drug concentration in different body spaces such as plasma, blood, urine, cerebrospinal fluid, and tissues, and aims to describe the different phases encountered by the compound once in the body: absorption, distribution, metabolism and elimination. The representation of the body is approximated by simple compartment models, each describing one body spaces, with the kinetics of the drug described by differential equations.
Suppose data from N = 6 subjects is available with the drug given orally. Figure 1.3 shows the concetration-time profiles of the different individuals: it can be seen the similiraty in shapes across subjects, but peaks, rises, decays vary considerably. This effect is attributable to *inter-subject variation* in underlying PK processes. Assuming a One-Compartment model with oral dose D (see Figure 1.4) given at time $t = 0$ leads to describe concentration $C(t)$ at time $t \geq 0$ as

$$C(t) = \frac{Dk_a}{V(k_a - \frac{Cl}{V})} \left[e^{-\frac{Cl}{V}t} - e^{-k_a t} \right]$$

where

- k_a: fractional rate of absorption $[1/Hr]$ of the drug from the gut compartment
- Cl: clearence rate $[ml/Hr]$, i.e. the volume of plasma which per unit of time is totally cleared of a substance (e.g. a drug) by the various elimination processes (metabolism and excretion)
- V: volume of distribution $[ml]$, i.e. the theoretical volume that a drug would have to occupy (if it was uniformly distributed), to provide the same concentration as it currently is in blood plasma

summarize the PK processes underlying the observed concentration profile of a given subject.

The final goal of a PK analysis is to determine the population mean values of (k_a, Cl, V) and how they vary between subjects, elucidating whether part of this variation is associated with subject characteristics (i.e. covariates, such as weight, age, renal function), in order to develop dosing strategies for subpopulations with certain characteristics (elderly, pediatric, etc.).
With respect to the model formulation encountered in 1.3.1, a correlation with the quantities in play leads to

1. Individual Model
    - $z_{i,j}$ is the drug concentration for subject i at time $t_{i,j}$, that is $z_{i,j} = C(t_{i,j})$

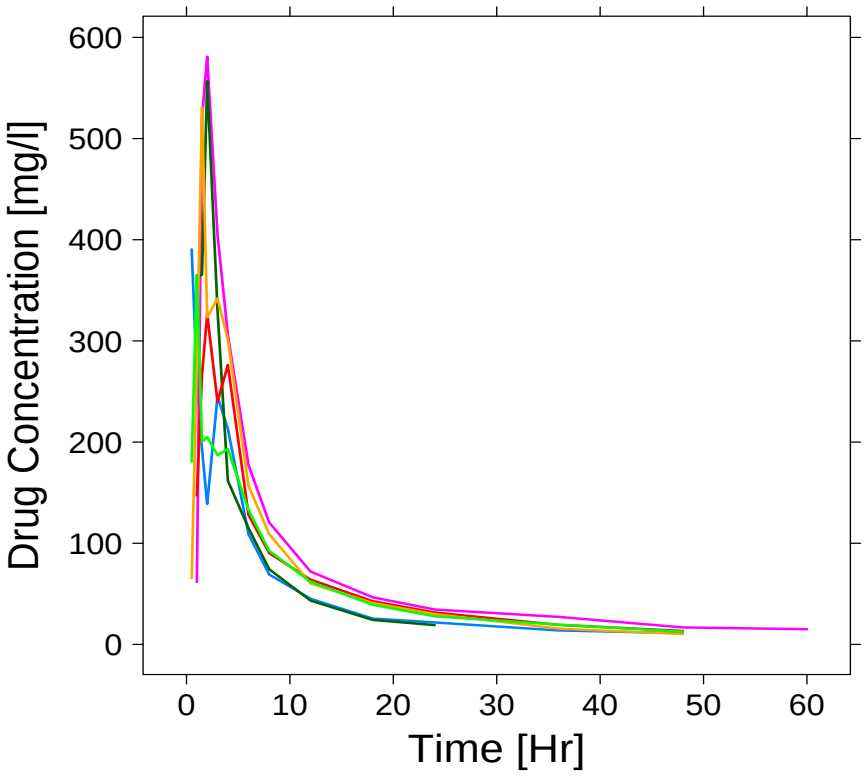

Figure 1.3: Example of drug concentration profiles after oral administration (each color identifies a single subject).

- $\mathbf{u}_i$ is the dose given to subject i a time $t = 0$, that is $\mathbf{u}_i = D_i$
- $\mathbf{p}_i$ are the PK parameters (k_a, Cl, V) specific to subject i, i.e. $\mathbf{p}_i = (k_{a_i}, Cl_i, V_i)$
- $f(\mathbf{t}_i, \mathbf{u}_i, \mathbf{p}_i)$ describes how the concentration of the i^{th} subject evolves in time in a one-compartment model with first order absorption, i.e.

$$f(\mathbf{t}_i, \mathbf{u}_i, \mathbf{p}_i) = \frac{D_i k_{a_i}}{V_i(k_{a_i} - \frac{Cl_i}{V_i})} \left[e^{-\frac{Cl_i}{V_i}\mathbf{t}_i} - e^{-k_{a_i}\mathbf{t}_i} \right]$$

2. Population Model

- $\mathbf{a}_i = \begin{bmatrix} G_i & BW_i \end{bmatrix}^T$, where G_i and BW_i are the gender and the body weight of subject i respectively

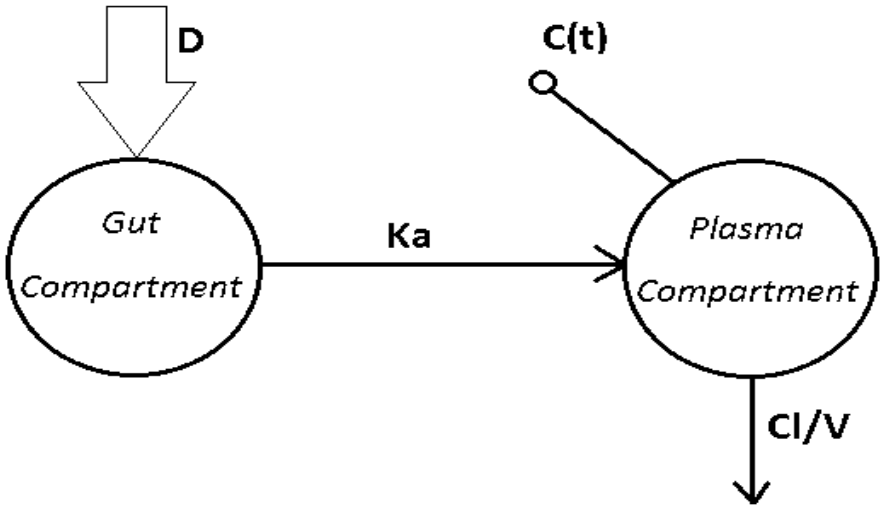

Figure 1.4: One compartment model with first order absorption from the gut compartment. Such model allows to take into account oral administration.

- $\boldsymbol{\eta}_i = \begin{bmatrix}\eta_{1,i} & \eta_{2,i} & \eta_{3,i}\end{bmatrix}^T$

$$\boldsymbol{\eta}_i \sim \mathcal{N}(\mathbf{0}, \boldsymbol{\Omega}), \boldsymbol{\Omega} = \begin{bmatrix}\omega_{11}^2 & \omega_{12}^2 & \omega_{13}^2 \\ \omega_{21}^2 & \omega_{22}^2 & \omega_{23}^2 \\ \omega_{31}^2 & \omega_{32}^2 & \omega_{33}^2\end{bmatrix}$$

  where $diag(\boldsymbol{\Omega})$ quantifies the varaibaility accross individuals of (k_a, Cl, V), respectively.

- $\boldsymbol{\theta} = \begin{bmatrix}\theta_1 & \theta_2 & \theta_3 & \theta_4\end{bmatrix}^T$
- The $\mathbf{d}$ function is the one that relates (k_{a_i}, Cl_i, V_i) to $(\mathbf{a}_i, \boldsymbol{\eta}_i, \boldsymbol{\theta})$, for example:

$$k_{a_i} = \theta_1 \cdot e^{\eta_1}$$

$$Cl_i = (\theta_2 + G_i \cdot \theta_3) \cdot e^{\eta_2}$$

$$V_i = (BW_i \cdot \theta_4) \cdot e^{\eta_3}.$$

In the pharmacokinetic context the use of exponentials on random effects $\boldsymbol{\eta}_i$ is required becuase of dealing with physiological entities, which are positive by implication. In addition, in the formulas above, an influence of the gender on the clearance and an influence of the body weight on the volume of distribution is assumed.

1.4 Basics of Bayesian Estimation

In the branch of estimation theory, Bayesian approach refers to the situation in which the information available comes from two different sources. Defining $\mathbf{y}$ as the observed data and $\boldsymbol{\theta}$ as the quantity to be estimated (a vector of parameters, a signal, etc.), these two founts are:

- **Likelihood**: the knowledge on the relationship between $\mathbf{y}$ and $\boldsymbol{\theta}$, denoted as $p(\mathbf{y}|\boldsymbol{\theta})$;
- **Prior**: the probabilistic a priori information on $\boldsymbol{\theta}$, denoted as $p(\boldsymbol{\theta})$;

thus, both $\mathbf{y}$ and $\boldsymbol{\theta}$ are treated as random variables.
Bayes theorem (equation (1.4)) enables to combine these two probability densities in order to obtain the so-called *posterior* density function $p(\boldsymbol{\theta}|\mathbf{y})$:

$$p(\boldsymbol{\theta}|\mathbf{y}) = \frac{p(\mathbf{y}|\boldsymbol{\theta})p(\boldsymbol{\theta})}{p(\mathbf{y})} \tag{1.4}$$

Translating the theorem in practical term: $p(\boldsymbol{\theta})$ represents the prior knowledge we have on the quantity to be estimated, if such quantity is somehow related to data $\mathbf{y}$, the observation of $\mathbf{y}$ (i.e. $p(\mathbf{y}|\boldsymbol{\theta})$) changes our expectations on $\boldsymbol{\theta}$ in $p(\boldsymbol{\theta}|\mathbf{y})$. In other words, by applying Bayes theorem we are extracting the estimate by way of a compromise between our knowledge on the quantity to be estimated and what the data is telling us (see Figure 1.5).
It is easy now to deduce the main difference between Bayesian inference and other approaches: through Bayes theorem the entire distribution of the parameters of interest can be estimated, providing a great amount of information. In fact, the use of posterior distribution is indeed wide, both because there are different ways to obtain the point-estimator of the parameter (such as the posterior mean, the posterior median or the posterior mode) and because it provides the credible intervals, which are a reliable measure (compared to confidence intervals used in frequentist approach) of the uncertainty of an estimate.
In order to be able to evaluate the postierior density function, Bayes theorem of equation (1.4) can be rewritten, using the "Law of Total Probability", as

$$p(\boldsymbol{\theta}|\mathbf{y}) = \frac{p(\mathbf{y}|\boldsymbol{\theta})p(\boldsymbol{\theta})}{\int_\theta p(\mathbf{y}|\boldsymbol{\theta})p(\boldsymbol{\theta})d\boldsymbol{\theta}}. \tag{1.5}$$

The denominator of equation (1.5) is a constant and does not depend on $\boldsymbol{\theta}$; hence, in the intereset of simplifying the formula as much as possible, we may consider

$$p(\boldsymbol{\theta}|\mathbf{y}) \propto p(\mathbf{y}|\boldsymbol{\theta})p(\boldsymbol{\theta}) \tag{1.6}$$

Unfortunately, only in a few particular cases $p(\boldsymbol{\theta}|\mathbf{y})$ is available in closed form, that is when the prior and the posterior come from the same family of distributions, and in this

case the prior is said to be conjugate to the likelihood. Example 1.4.1 shows one of these cases.

Example 1.4.1. Let us consider a drug to be given for relief of chronic pain whose experience with similar compounds has suggested that annual response rates between 0.2 and 0.6 could be feasible, then we may interpret this as a distribution with mean = 0.4 and standard deviation = 0.1. Suppose we now treat n = 20 volunteers with the compund and observe y = 15 positive responses.

- *Likelihood*. Assuming patients are independent, with common unknown response rate θ, leads to a binomial likelihood (Figure 1.5a):

$$y \sim Binomial(\theta, n)$$

$$p(y|n,\theta) = \binom{n}{y}\theta^y(1-\theta)^{n-y} \propto \theta^y(1-\theta)^{n-y}$$

- *Prior*. A probability distribution which fits with the requests on the response rate is a Beta distribution (with a=9.2 and b=13.8, see Figure 1.5b):

$$\theta \sim Beta(a,b)$$

$$p(\theta) = \frac{\Gamma(a+b)}{\Gamma(a)\Gamma(b)}\theta^{a-1}(1-\theta)^{b-1} \propto \theta^{a-1}(1-\theta)^{b-1}$$

- *Posterior*. Combining the Binomial likelihood and the Beta prior gives the following posterior distribution

$$p(\theta|y,n) \propto p(y|\theta,n)p(\theta)$$

$$p(\theta|y,n) \propto \theta^y(1-\theta)^{n-y}\theta^{a-1}(1-\theta)^{b-1} = \theta^{y+a-1}(1-\theta)^{n-y+b-1}$$

  which is still a Beta dsitribution (with different parameters, see Figure 1.5c):

$$p(\theta|y,n) \propto Beta(y+a, n-y+b)$$

In most cases $p(\boldsymbol{\theta}|\mathbf{y})$ is not analitically tractable and we want to obtain the marginal posterior $p(\theta_i|\mathbf{y})$ for each i and calculate properties of $p(\theta_i|\mathbf{y})$ such as the mean ($\int \theta_i p(\theta_i|\mathbf{y})d\theta_i$) and the tail areas ($\int_T^\infty p(\theta_i|\mathbf{y})d\theta_i$). Given that evaluating these integrals analitically is impossible, numerical integration becomes vital. WinBUGS [6] is a free software that allows to obtain every $p(\theta_i|\mathbf{y})$ and compute integrals on them via Markow Chain Monte Carlo (MCMC) techniques.

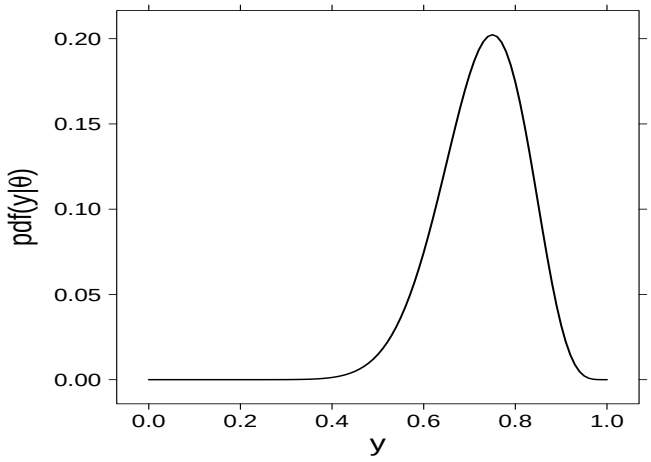

(a)

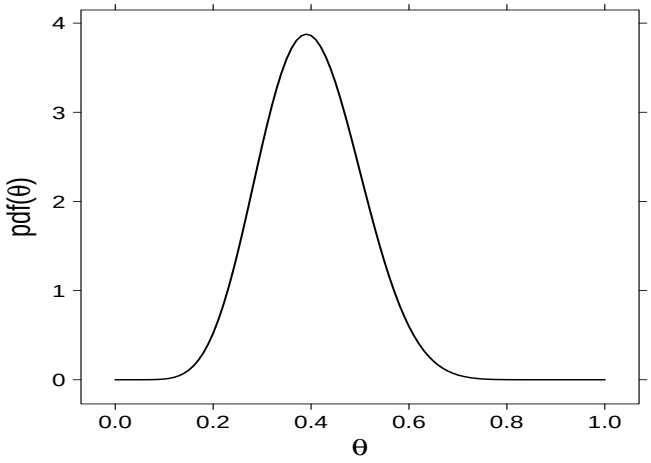

(b)

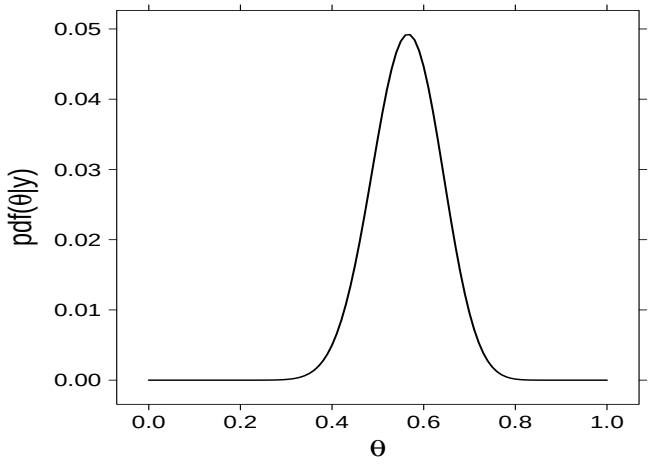

(c)

Figure 1.5: Probability density function (up to a multiplicative constant) of: Likelihood (a), Prior (b) and Posterior (c) defined in example 1.4.1. It may be noticed how the posterior obtained would be in the middle (a compromise) between the prior and the likelihood.

Chapter 2

Materials and Methods

2.1 Preclinical Protocol

2.1.1 Pharmacokinetic Data

The compound (GSK945237) was administered orally twice daily (*Bis In Die*, i.e. BID) with approximately 6 hours between doses to nine male and nine female beagle dogs (total number of individuals=18) at total daily doses of 0, 30, 100 and 300 mg/kg/day (0, 15, 50 and 150 mg/kg/day BID, respectively). Plasma samples were obtained from blood collected into tubes containing EDTA from drug-treated and placebo-control animals at the following nominal times: predose, 0.25, 0.5, 1, 3, 6, 6.25, 6.5, 7, 9 and 24 hours after the first dose.
Plasma samples were analyzed for GSK945237 using a validated analytical method based on protein precipitation, followed by HPLC-MS/MS analysis. Using a 50 μL aliquot of dog plasma, the lower limit of quantification (LLQ) for GSK945237 was 0.1 ng/L and the higher limit of quantification (HLQ) was 50 ng/L.

2.1.2 Pharmacodynamic Data

Four male dogs were given placebo and total daily doses of 30, 100 and 300 mg/kg (15, 50 and 150 mg/kg administered twice daily approximately 6 hours apart) of test article orally by gavage on separate days, with at least 7 days between each dose, according to a 4x4 latin square crossover paradigm. Dogs were dosed at approximately 9:00 AM on each day of dosing. ECG waveforms were recorded continuously from 2 hours prior to dosing to 24 hours after dosing and all derived parameters were recorded as 1-minute means.
According to the aim of the analysis and given the enormous amount of data collected overall, raw QT data was diluted every 2 minutes during the absorption phase (roughly $t<2.5$hrs and $6\text{hrs}<t<8.3$hrs, where t is the time after dosing), every 5 minutes during the distribution phase ($2.3\text{hrs}<t<6$hrs and $8.3\text{hrs}<t<15$hrs) and every 15 minutes during

the elimination phase (t>15hrs). Also, part of the ECG data collected around the dosing times had to be discarded due to the bad quality of the data caused by an abnormal dogs excitement.

2.2 Clinical Protocol

2.2.1 Pharmacokinetic-Pharmacodynamic (PK-PD) Data

The study was a first-time-in-human to investigate the safety, tolerability, and pharmacokinetics of escalating single oral doses of GSK945237. The adopted design was a single-blind, randomized, placebo-controlled, dose-rising study conducted in sequential cohorts. Forty-five (45) subjects were enrolled into 6 cohorts. According to a randomization schedule prepared prior to study start, 6 subjects received active drug and 3 subjects received placebo at each dose level (50mg, 150mg, 400mg, 1000mg, 2000mg and 2600mg). Each subject participated in one study period and received either GSK945237 or matching placebo.
Following a single oral dose of GSK945237, blood samples for pharmacokinetic analysis and ECG waveform samples for pharmacodynamic analysis of GSK945237 were collected over a 60-hour period from groups receiving doses of 50mg, 250mg and 500mg and over a 120-hour period from groups receiving 1000mg and 1750mg. Bioanalysis of GSK945237 plasma concentrations was conducted using a validated analytical method based on solid phase extraction followed by HPLC-MS/MS. The lower limit of quantification (LLQ) for GSK945237 was 10 ng/mL, using a 100 L aliquot of human plasma with a higher limit of quantification (HLQ) of 5000 ng/mL.

2.3 Pharmacokinetic Modelling

The goal of the pharmacokinetic (PK) modelling in the whole project is to obtain time matched concentration and QT interval values, since this is required for the assessment of the pharmacokinetic-pharmacodynamic (PK-PD) relationship. In order to do this, PK modelling has been performed using non-linear mixed effect techniques (see 1.3.2 for an example) implemented in NONMEM 7.1.2 [7]. Once identified the best PK model for GSK945237, the parameter estimates obtained are used to generate simulated concentration profiles with the same sampling time used to collect QT measurements.
Since in human data QT measurements and concentration measurements were collected simultaneously, the PK step was executed only for conscious dogs data, where the QT sampling time is usually low (30 sec/1 min) and therefore an equal PK sampling time is not achievable for obvious reasons.
Firstly, provided that the drug administration was oral, a model with first order absorption had to be taken into account. Secondly, the BID way of administration made it difficult to describe the data after the second daily dose since the dogs had free access to food between

the two daily doses, determining the appearaence of a food effect in the data. Finally, the NONMEM analysis led to the conclusion that a one compartment model with first order absorption (Fig.1.4) best decribes the kinetic of the analyzed drug.

2.3.1 NONMEM Model Formulation

The mandatory parameters for a one compartment model with first order absorption are: Rate of Absorption (K_a), Clearance (Cl) and Volume of Distribution (V). Bioavailability (F) was also included in the model in order to describe the food effect.
After a covariate analysis, it emerged that the Clearance and the Volume of Distribution are affected by the gender and the body weight of the individuals, respectively.
The detailed model formulation is (t represents the time variable):

$$FE_{Cl} = \begin{cases} \theta_1 & \text{if GENDER=M} \\ \theta_2 & \text{if GENDER=F} \end{cases} \implies Cl = FE_{Cl} \cdot e^{\eta_1}$$

$$V = WT \cdot \theta_3 \cdot e^{\eta_2}$$

$$FE_{K_a} = \begin{cases} \theta_4 & \text{if First Daily Dose (FDD)} \\ \theta_5 & \text{if Second Daily Dose (SDD)} \end{cases} \implies K_a = FE_{K_a} \cdot e^{\eta_3} \tag{2.1}$$

$$F = \begin{cases} \theta_6 & \text{if DOSE=30 mg/kg and DOSE=SDD} \\ \theta_7 & \text{if DOSE=300 mg/kg and DOSE=FDD} \\ \theta_8 & \text{if DOSE=300 mg/kg and DOSE=SDD} \\ 1 & \text{otherwise} \end{cases} \tag{2.2}$$

The residual error model that has produced the lowest objective function value is a mixed (proportional and addittive) one:

$$Y = f(\boldsymbol{\theta}, \boldsymbol{\eta}, \boldsymbol{t}) \cdot (1 + \epsilon_1) + \epsilon_2 \tag{2.3}$$

where Y is the observed concentration, $f(\boldsymbol{\theta}, \boldsymbol{\eta}, \boldsymbol{t})$ the predicted concentration, $\epsilon_1 \sim \mathcal{N}(0, \sigma_1^2)$ and $\epsilon_2 \sim \mathcal{N}(0, \sigma_2^2)$.

2.4 PK-PD Modeling of the QT interval

The aim of this section is to define a mathematical model able to decribe the QT interval. Since there are different sources contributing on QT variation, each of them is explored.

2.4.1 Modelling the Drug Effect

Pharmacodynamics can be defined as the relationship between the drug concentration in the plasma and the pharmacological effect. In order to be able to characterize this relationship and quantify the drug response, various mathematical models are available [8]. Among those, the one that has been implemented is a linear concentration-effect model (Figure 2.1)

$$E = E_0 + S \cdot C \tag{2.4}$$

where E indicates the drug effect, E_0 the baseline effect, C the plasmatic concentration of the drug and S the slope parameter.

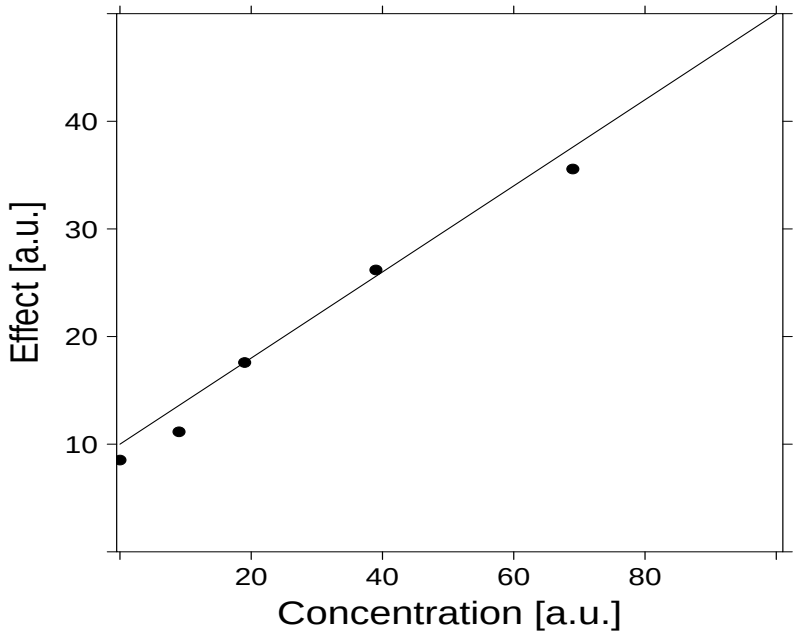

Figure 2.1: Observed effect (dots) versus concentration described by a linear model (solid line).

Despite an ordinary E_{max} model (Figure 2.2)

$$E = E_0 + \frac{E_{max} \cdot C}{EC_{50} \cdot C} \tag{2.5}$$

(where EC_{50} denotes the plasma concentration corresponding to the half-maximal difference between baseline E_0 and the maximal effect E_{max}) might be more physiologically plausible as it takes into account the maximum effect, the range of concentration values involved in QT studies does not determine any saturation effects, allowing the use of a

linear model.

In the context of QT variation, equation (2.4) can be rewritten as

$$\Delta QT_{DE} = Slope \cdot C \tag{2.6}$$

where ΔQT_{DE} represents the variation of the QT interval due to the drug effect and the unit of measurement of the *Slope* will be $[ms/concentration]$. The baseline effect E_0 will be consider in section 2.4.2.

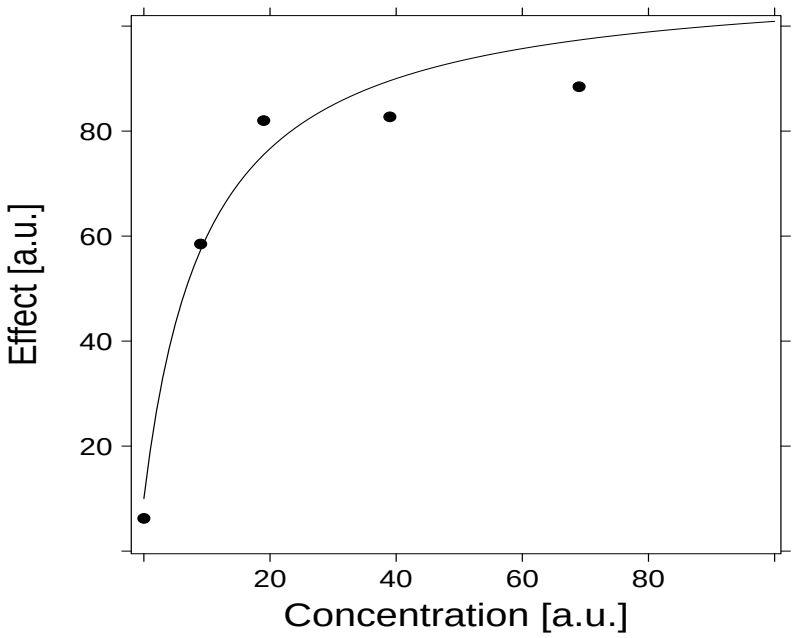

Figure 2.2: Observed effect (dots) versus concentration described by an E_{max} model (solid line).

2.4.2 Modelling the QT-RR Relationship

It has been already mentioned that the QT interval depends on the RR one, but how are they related? Since 1920 when two pioneering article appeared [9],[10], many efforts have been made to find a formula that provides the ideal correction such that the corrected QT interval is indipendent of the RR interval.
The most used formulas so far are the so-called Bazett correction [9]

$$QTc_B = QT \cdot RR^{-0.5} \tag{2.7}$$

and Friedericia correction [10]

$$QTc_F = QT \cdot RR^{-0.33} \tag{2.8}$$

where QT is in $[ms]$ and RR is in $[s]$ (there is no a scientific reason why RR and QT have two different measurement units in these formulas, on the contrary, it came out from empirical evidence). Figure 2.3 compares the two formulas using as an example a pooled dataset comprising QT-RR measurements from 45 individuals. Between the two formulas, that of Friedericia (Figure 2.3b) performs on avarage quite well (the loess smoother is almost horizontal), while Bazett formula (Figure 2.3a) determines an over-correction.
Despite the good behaviour of Friedericia's formula, equations (2.7) and (2.8) have been derived from population data, and the large difference between these formulae suggests that the QT/RR relationship has not been found reproducible from study to study. It is therefore unreasonable to expect that a general formula could satisfy the QT/RR relationship for the data of a given study, namely, individuals show different QT/RR relationships. Keeping the same template of equations (2.7) and (2.8), the QTc baseline interval (QTc_0) can be described as

$$QTc_0 = QT_0 \cdot RR^{-\alpha} \tag{2.9}$$

where QT_0 is the measured QT baseline interval. Now, given that the aim is to describe the QT interval, equation (2.9) has to be rewritten as

$$QT_0 = QTc_0 \cdot RR^{\alpha} \tag{2.10}$$

A population approach makes possible to estimate every individual correction factor α_i obtaining a population parameter α denoting the QT correction factor for the population recruited in the specific study. Furthermore, QT_0 in equation (2.10) plays the role of the baseline effect E_0 introduced in equation (2.4) which was lacking in equation (2.6).

2.4.3 Modelling the Circadian Rhythm

As mentioned in section 1.1, the QT interval depends on several factors. Obviuosly, trying to build a model able to describe each of them would be too complex as well as without any pharmacological interest. Amongst the elements influencing the QT, apart from the aforementioned RR interval and drug effect, the circadian rythm is one of the most sizable (see Figure 2.4).

In general, the statistical significance of the circadian rythmicity can be documented by the cosinor analysis [11], [12]. This method characterizes a rhythm by the parameters of a fitted cosine function

$$\Delta QT_{circ} = A \cdot cos\left[\frac{2\pi}{24}(t_c - \phi)\right] \tag{2.11}$$

where ΔQT_{circ} denotes the variation in milliseconds of the QT interval due to the circadian rythm, A $[ms]$ and ϕ $[hr]$ are its amplitude and phase respectively and t_c is the clock time.
The ability to estimate the crircadian component is limited by the number of QT interval measurements available and their spread over the day. In fact, since the precision of QT data is low, a large number of observations is needed to extract a signal coming from the circadian ryhtm.

Concluding, the final model may be obtained by gathering each of the single contributes described so far, i.e. the drug effect (equation (2.6)), the QT/RR relationship (equation (2.10)) and the circadian rythm (equation (2.11)), that is, $QT = QT_0 + \Delta QT_{circ} + \Delta QT_{DE}$, which leads to

$$QT = QTc_0 \cdot RR^{\alpha} + A \cdot cos\left[\frac{2\pi}{24}(t_c - \phi)\right] + Slope \cdot C \tag{2.12}$$

2.4.4 WinBUGS Model Formulation

The PK-PD model of equation (2.12) has been implemented in WinBUGS via a hierarchical model which allows to take into account different sources of variability, as well as prior distributions (Figure 2.5).

The detalied formulation is the following (hereafter: $i = 1, ..., N$ individuals, $k = 1, ..., P$ occasions and $j = 1, ..., M$ time samples)

$$QT_{i,k,j} = f_{k,j}(\mathbf{p}_i) + \epsilon_j \tag{2.13}$$

where ϵ_j is the measurement error, at time j, assumed normally distributed ($\epsilon_j \sim \mathcal{N}(0, \sigma_\epsilon^2)$) and

$$f_{k,j}(\mathbf{p}_i) = QTc_{0_{i,k}} \cdot RR_{i,j}^{\alpha_i} + A_i \cdot cos\left[\frac{2\pi}{24}(t_{c_j} - \phi_i)\right] + Slope_i \cdot C_{i,j} \tag{2.14}$$

is the direct translation of equation (2.12).

Carrying on with the fromulation, $\mathbf{p}_i$ is a vector of individual parameters

$$\mathbf{p}_i = \begin{bmatrix} p_{1,i} & p_{2,i} & p_{3,i} & p_{4,i} & p_{5,i} \end{bmatrix}^T$$

which will be used to derive the actual parameters appearing in the model and follows a multivariate normal distribution (MVN)

$$\mathbf{p}_i \sim \mathcal{MVN}(\boldsymbol{\theta}, \boldsymbol{\Omega})$$

where

$$\boldsymbol{\theta} = \begin{bmatrix} \theta_1 & \theta_2 & \theta_3 & \theta_4 & \theta_5 \end{bmatrix}^T$$

represents the vector of the fixed-effects and

$$\mathbf{\Omega} = \begin{bmatrix} \omega_{11}^2 & \omega_{12}^2 & \omega_{13}^2 & \omega_{14}^2 & \omega_{15}^2 \\ \omega_{21}^2 & \omega_{22}^2 & \omega_{23}^2 & \omega_{24}^2 & \omega_{25}^2 \\ \omega_{31}^2 & \omega_{32}^2 & \omega_{33}^2 & \omega_{34}^2 & \omega_{35}^2 \\ \omega_{41}^2 & \omega_{42}^2 & \omega_{43}^2 & \omega_{44}^2 & \omega_{45}^2 \\ \omega_{51}^2 & \omega_{52}^2 & \omega_{53}^2 & \omega_{54}^2 & \omega_{55}^2 \end{bmatrix}$$

depicts the random-effect component, i.e. the Between Subject Variabilty (BSV) of the parameters.
The parameters of equation (2.14) are expressed as follows:

$$QTc_{0_{i,k}} = e^{p_{i,1}+\lambda_k} \tag{2.15}$$

where the variable λ_k is normally distributed around 0 with variance σ_λ^2 (i.e. $\lambda_k \sim \mathcal{N}(0, \sigma_\lambda^2)$) and has been introduced in order to take into account the variability of the baseline QTc across study periods (the baseline QTc varies from day to day). Such a source of variabilty is called Inter-Occasion Variability (IOV). Furthermore, as the QTc_0 is a physiological parameter and therefore can not be negative, we make sure it will assume only positive values by taking the exponent of $p_{i,1} + \lambda_k$.

$$\alpha_i = e^{p_{i,2}}$$

It has already been described how the RR affects the QT interval (see section 2.4.2). In particular, from equation (2.10), we know that the parameter α has to be positive. This is the reason why the exponent of $p_{i,2}$ was considered.

$$A_i = e^{p_{i,3}}$$

$$\phi_i = e^{p_{i,4}}$$

A and ϕ are the model parameters used to describe the circadian component of the QT interval. Theoretically, the sign of these two parameters is arbitrary, therefore no positive constrains should be adopted. However, from a practical point of view, i.e. in order to narrow the optim parameters searching field, exponential terms were considered, forcing A and ϕ to be positive. With the aim of being able to assert that this choice does not affect the parameters' estimate, a model run with a negative constrain on A was performed (i.e. $A_i = -e^{p_{i,3}}$). Results shown in Figure 2.6 enable to draw the conclusion that the model recognizes the fact that the amplitude cannot be positive, and in consequence shifts the phase ϕ to a value 12Hr greater than the previous one, thereby obtaining the same overall estimate of the cyrcadian rhythm component.

$$Slope_i = 10^{-5} \cdot p_{i,5} \tag{2.16}$$

The formulation of *Slope* showed above contains a multiplication by 10^{-5}, whose goal comes from numerical issues. Since *Slope* parameter is known to be low, equation (2.16) ensures that $p_{i,5}$ will be a reasonable high number, supporting the algorithm in finding a solution.

Priors Choice The selection of a prior for a given parameter is, in principle, subjective: it might be elicited from experts, it might be based on historical data (e.g. a previous study) or it might be convenient to assume a vague, non-informative prior.
As to priors on σ_ϵ^2 and σ_λ^2, a Jeffrey's prior on the inverse of these two quantities is a standard choice if no a-priori information is present on them (non-informative prior):

$$\frac{1}{\sigma_\epsilon^2} \sim Gamma(\delta, \delta)$$

$$\frac{1}{\sigma_\lambda^2} \sim Gamma(\delta, \delta)$$

where δ is an arbitrary small number (usually $\delta = 0.001$).
Concerning the parameters $\boldsymbol{\theta}$ and $\boldsymbol{\Omega}$, the choice was also for non-informative priors in order to do not bias the estimation too much. In particular, the priors were specified as:

$$\boldsymbol{\theta} \sim \mathcal{MVN}(\boldsymbol{\mu}, \boldsymbol{\Sigma})$$

where

$$\boldsymbol{\mu} = \begin{bmatrix} 0 \\ 0 \\ 0 \\ 0 \\ 0 \end{bmatrix}, \boldsymbol{\Sigma} = 10^4 \cdot \begin{bmatrix} 1 & 0 & 0 & 0 & 0 \\ 0 & 1 & 0 & 0 & 0 \\ 0 & 0 & 1 & 0 & 0 \\ 0 & 0 & 0 & 1 & 0 \\ 0 & 0 & 0 & 0 & 1 \end{bmatrix}$$

and

$$\boldsymbol{\Omega}^{-1} \sim \mathcal{W}p(\mathbf{R}, 5)$$

where $\mathcal{W}p(\mathbf{R}, \rho)$ indicates a Wishart distribution with scale matrix $\mathbf{R}$ and degrees of freedom ρ and it is a common choice for prior of the inverse covariance-matrix (i.e. $\boldsymbol{\Omega}^{-1}$) of a multivariate-normal random-vector (i.e. $\boldsymbol{\theta}$) since it is a conjugate prior for it [13]. To represent vague prior knowledge, ρ was set small as possible (i.e. 5, the rank of $\boldsymbol{\theta}$). Finally, the scale matrix was specified as

$$\mathbf{R} = \begin{bmatrix} 1 & 0 & 0 & 0 & 0 \\ 0 & 1 & 0 & 0 & 0 \\ 0 & 0 & 1 & 0 & 0 \\ 0 & 0 & 0 & 1 & 0 \\ 0 & 0 & 0 & 0 & 1 \end{bmatrix},$$

an arbitrary, as well as common, option given that the choice of $\mathbf{R}$ has little effect on the posterior estimate of $\mathbf{\Omega}$ [14].

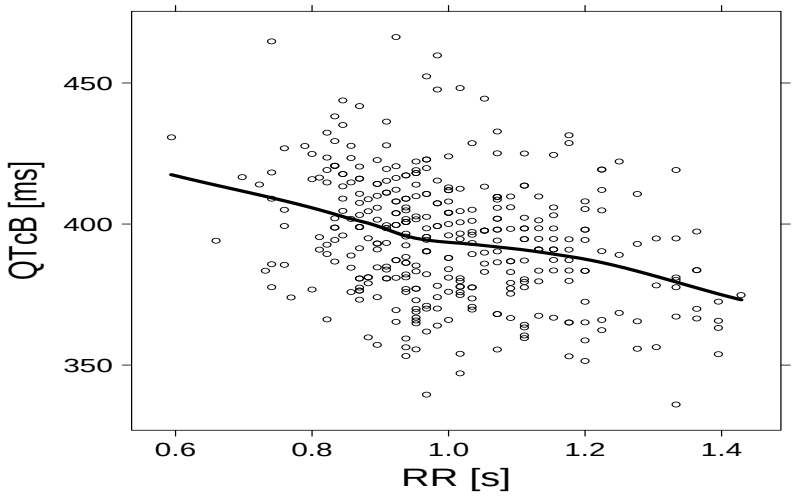

(a)

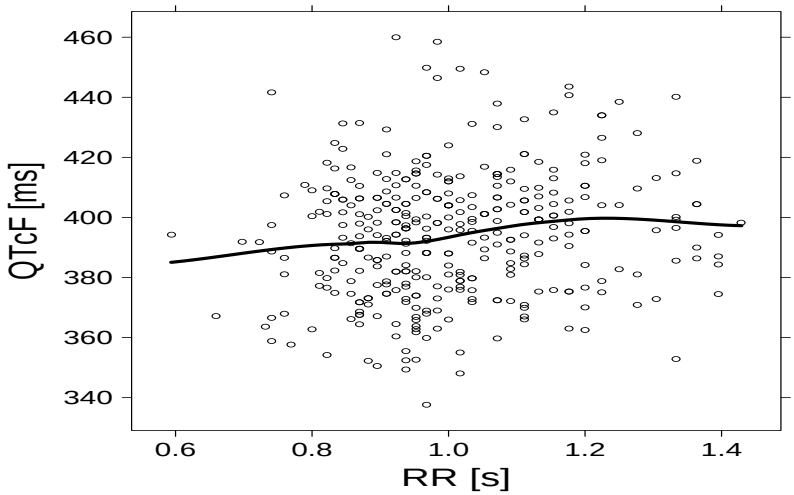

(b)

Figure 2.3: Comparision between the RR correction formulas of equations (2.7) and (2.8): (a) Bazett correction and (b) Friedericia correction. The dots represent the QTc measurements. The loess smoother (solid line) shows a better performance for Fridericia correction.

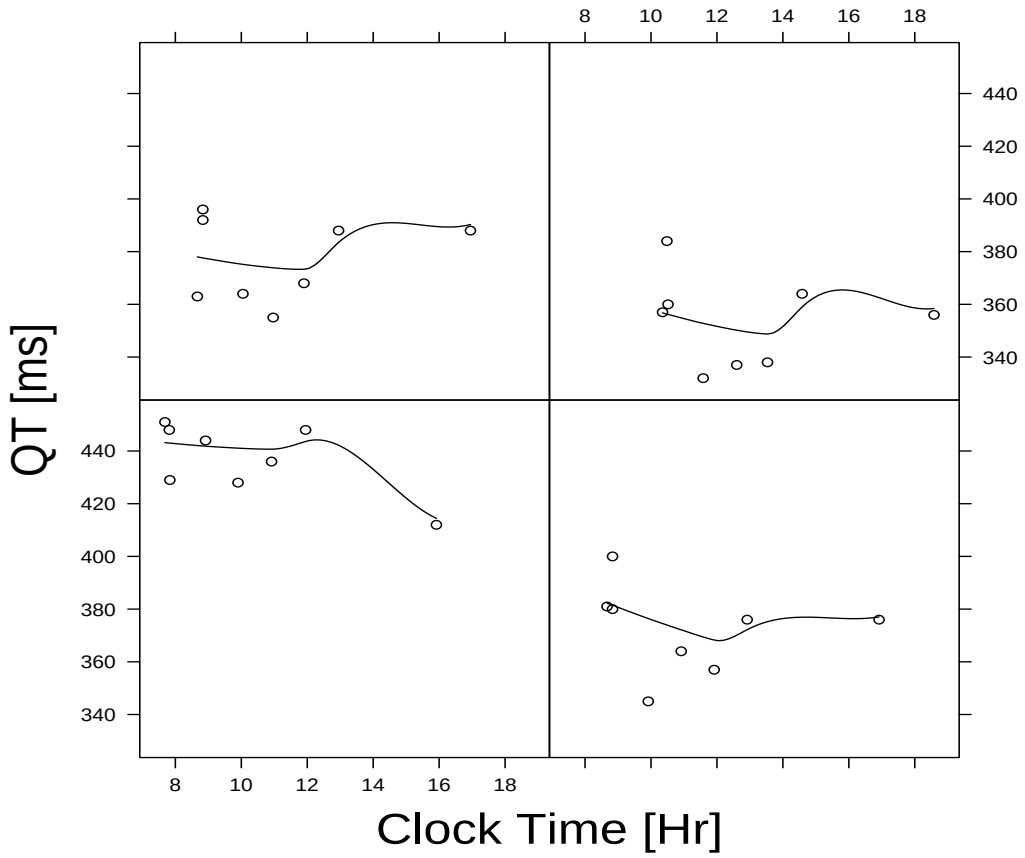

Figure 2.4: QT intervals (circles) measured in placebo groups vs clock time. The solid line is a loess smoother showing a circadian variation in the QT.

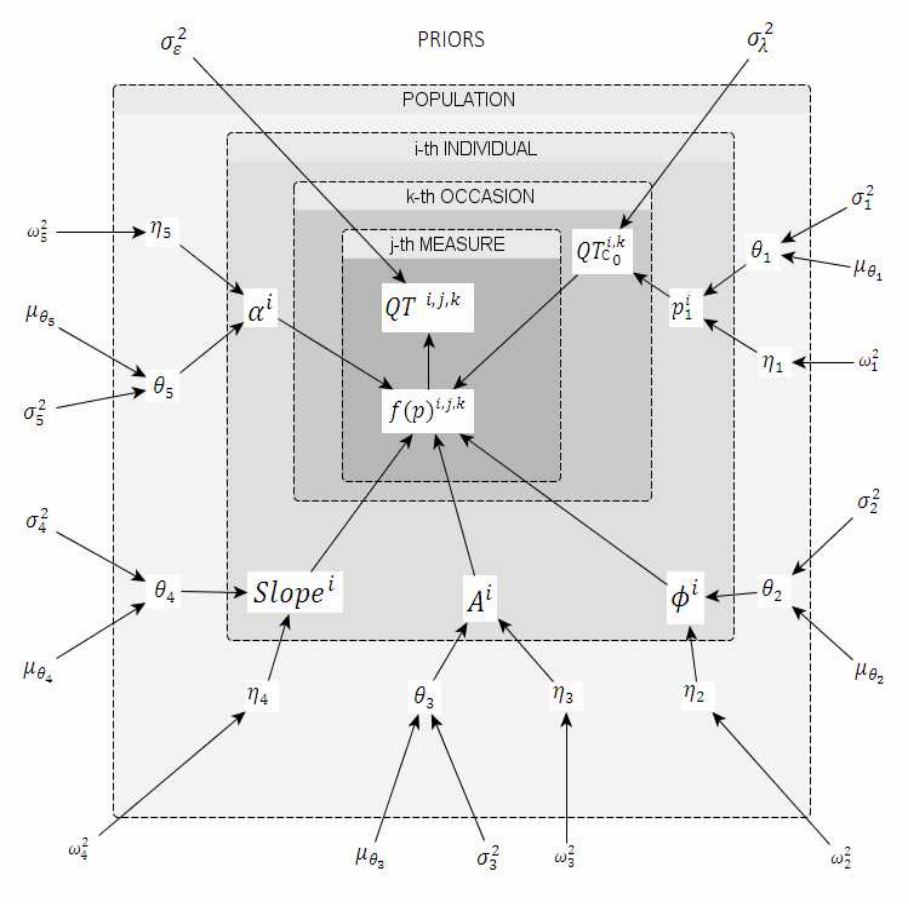

Figure 2.5: Graph of the hierarchical model used for the PK-PD analysis. The different levels are, from lower to higher: Prios level, Population level, Individual level, Occasion level and Measurement level.

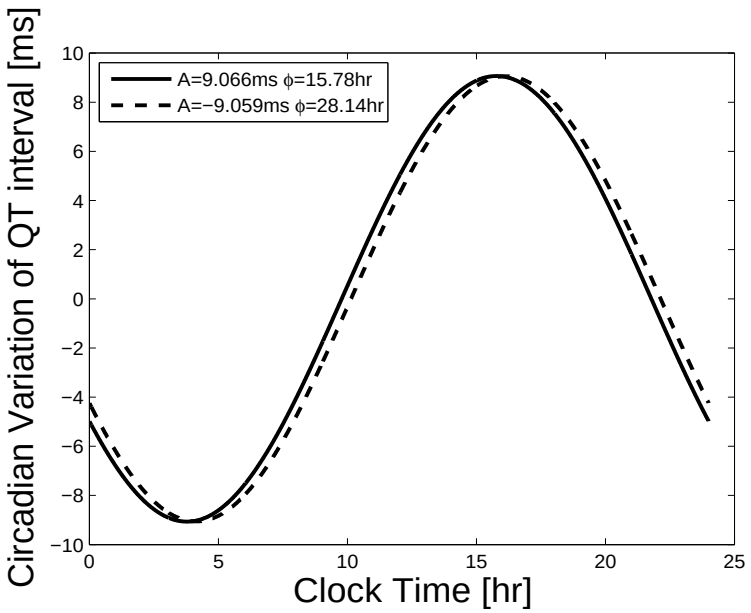

Figure 2.6: Comparison between the circadian rhythm estimated with a positive (solid line) and negative (dashed line) constrain on the amplitude.

Chapter 3

Results

3.1 Pharmacokinetic Analysis

3.1.1 Preclinical Data

In this section, results from the preclinical PK model of GSK945237 (described in section 2.3.1) will be presented and discussed. The outcomes will be interpreted through both a numerical and graphical point of view. All the estimates that are going to be documented were obtained in NONMEM adopting the pre-implemented Maximum Likelihood estimation algorithm called First Order Conditional Estimation (FOCE) with interaction.
A fair diagnostic plot to see how the model works at first glance is the so called Goodness of Fit (GOF) plot for population prediction (Figure 3.1). The population GOF plot aims to show the overall behaviour of the model, and the key point to interpret it is that the closer the black dots are to the unity line the better the prediction is, since this is proof of a good correlation between observed and predicted concentrations. The plot reveals a difficulty in getting the higher concentration values as there is a slight shift of the dots under the unity line for measured concentrations in between 23-30 ng/L. Nevertheless, given the small number of indivduals involved in the study (18), the model may be accepted and subjected to further examination. Figure 3.2 illustrates the GOF plot for individual predicted concentrations, which are obtained by way of a Maximum a Posteriori (MAP) Bayesian estimatation of the indivdual PK parameters using the population estimates as priors (this step is automatically done by NONMEM). In this case the correlation between predictions and observations is higher than in the population GOF, which is what one would expect since there is an individual prediction for every subject.
The residuals analysis is an alternative way to evaluate the goodness of a model. A residual is defined as the difference between the observed measure and the model prediction, therefore the lower the residuals are the better the prediction is; on the other hand, weighted residuals are residuals scaled by a certain weight parameter (for example the variance of the measurement error, if we have information on it) that quantifies the confidence we have

on a certain sample. Under certain statistical assumptions, in order to assess the goodness of the prediction, two particular features of the weighted residuals have to be checked: correlation (the more they are uncorrelated the better the fit is) and amplitude (they should be distributed around -1 and 1). Outcomes from such analysis are showed in Figure 3.3, and it can be seen the performance of the model is overall good, except for a sistematic bias in the last sample. Given the goal of the PK step though, since we are interested in higher concentrations and the model lacks on the last sample which is associated with a very low concentration value, this flaw may be neglected.

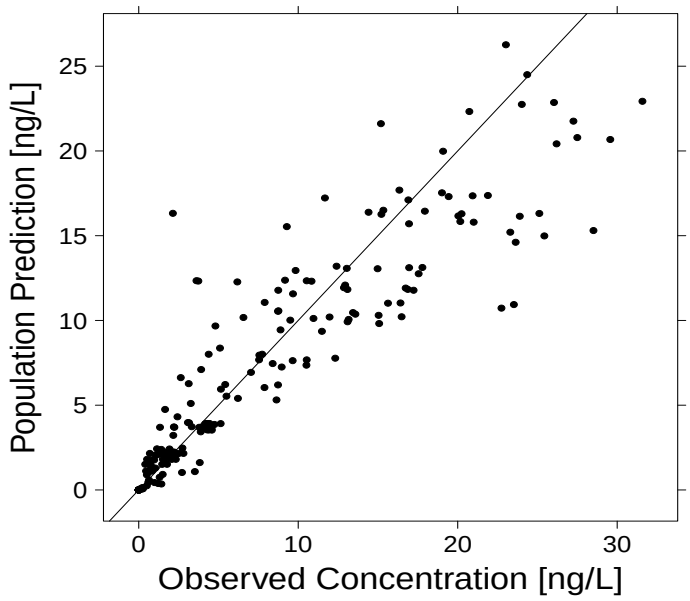

Figure 3.1: Goodness of Fit plot for the population preditced vs. observed drug concentration (the solid line depicts the unity line).

A more accurate diagnostic tool is represented by the Visual Predictive Check (VPC), which is mainly used to support the appropriateness of a model. The VPC is constructed from stochastic simulations of the model, therefore all the model components contribute and it can help in diagnosing both structural and stochastic contributions. In Figure 3.4 is portrayed the outcome from 1000 model's simulations where the 25^{th} and 75^{th} percentiles have been chosen due to the small size of the dataset [15]. The plot displays the capacity of the model to express the variabilty that exists among individuals, where the accuracy in doing that is confirmed by the fact that the measurements lying further the two percentiles are around the 25% of the whole dataset (Table 3.1).

Now that the goodness of the model has been established, all the parameter estimates may be explored.

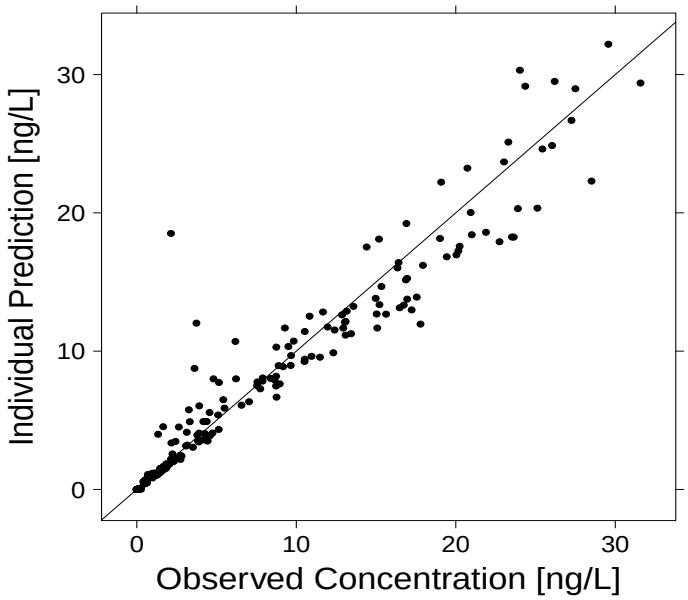

Figure 3.2: Goodness of Fit plot for the individual preditced vs. observed drug concentration (the solid line depicts the unity line).

Percentage of data above the 75th percentile	Percentage of data beneath the 25th percentile
28.8%	24.7%

Table 3.1

Table 3.2 contains the estimates (with their coefficient of variations) of the fixed effects of the model. Referring to Figure 3.5 and the values obtained for θ_4 and θ_5, it should be appear clear why the K_a has been formulated as in equation (2.1): mostly due to the food effect, the rate of absorption of the first daily dose is rather higher than the one in the second dose. Also, as it may seen from the large variability in the second peak between Figures 3.5a, 3.5b and 3.5c, the fact that dogs were fed between the two daily doses has an influence in the maximum concentration of the second daily dose as well, depending on the amount of drug administered. In the interest of making the model sensitive to such effect, three different bioavailabilities for the three different dose regimens (30, 100 and 300 mg/kg) were taken into account (equation (2.2)), where the "full bioavailabilty" (i.e. $F = 1$) was assumed to be the one on the first daily dose and on the 100 mg/kg dosing regimen.

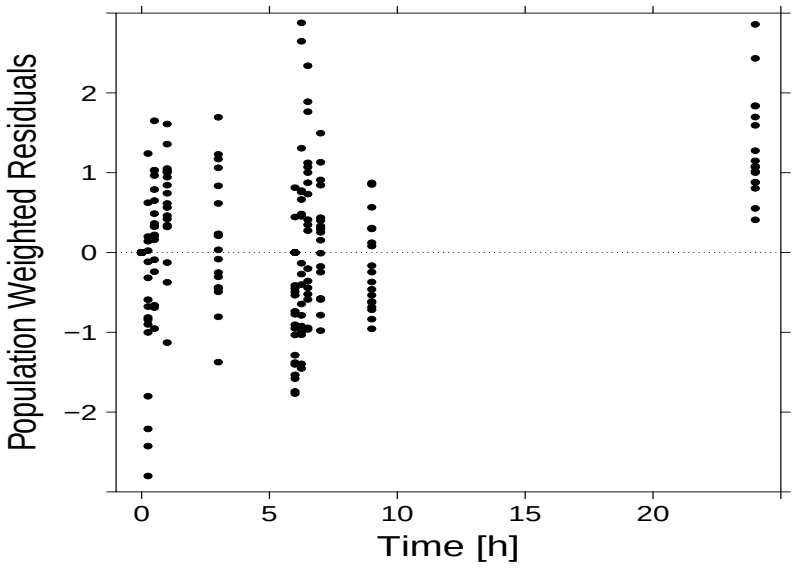

(a)

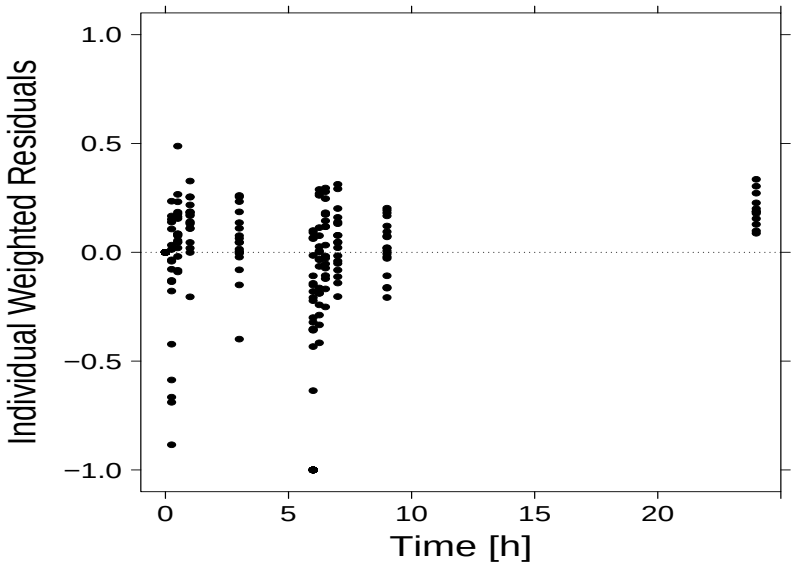

(b)

Figure 3.3: Population weighted residuals (a) and individual weighted residuals (b).

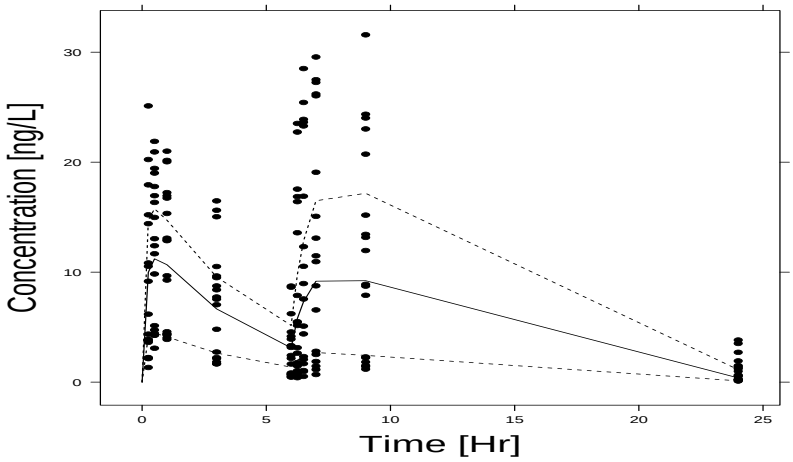

Figure 3.4: Visual Predictive Check of the PK model (1000 simulations). Dots: observed concentrations, solid line: median of the 1000 simulated profiles, dashed lines: 25th and 75th percentile of the 1000 simulated profiles.

	θ_1	θ_2	θ_3	θ_4	θ_5	θ_6	θ_7	θ_8
	$\left[\frac{L}{hr}\right]$		[L]	$\left[\frac{1}{hr}\right]$		unitless		
Value	6.34	4.51	3.45	8.59	0.789	0.609	0.44	0.78
CV (%)	10.1	8.8	7.1	20.8	23.4	9.7	11	12.5

Table 3.2: Estimates of the population mean parameters along with their precisions (expressed via percentage coefficient of variation) of the PK model.

Finally, the estimates of the random effects are proposed. As discussed in section 1.3.1, in the first place the random effects are associated with two sources of variability: Between Subject (Table 3.3) and Intra (Within) Subject (Table 3.5).
The estimates of the BSV in Table 3.3 are depicted by means of coefficients of variation, that is $BSV_n = \frac{\omega_n}{\theta_n}$, where ω_n is the true enitity that expresses the BSV of the n^{th} $(n = 1, 2, 3)$ parameter, but it is divided by the population mean in the interest of having a relative measure of the variability of that particular parameter. A further indicator of the goodness of the BSV estimates is the result of an hypothesis test on the values of η_n, assuming as null hypothesis that η_n has mean zero (see equation (1.3)). Table 3.4 summarizes the outcomes of this test, showing p-values that allow to accept the null hypothesis, i.e. all the η_n have mean zero, giving an additional evidence of the appropriateness of the proposed model.

Regarding the Intra Subject Variability (ISV) estimates of Table 3.5, the proportional

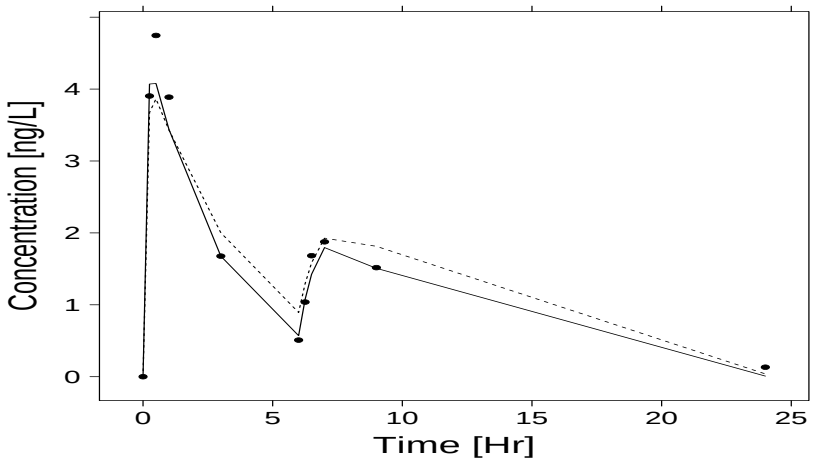

(a)

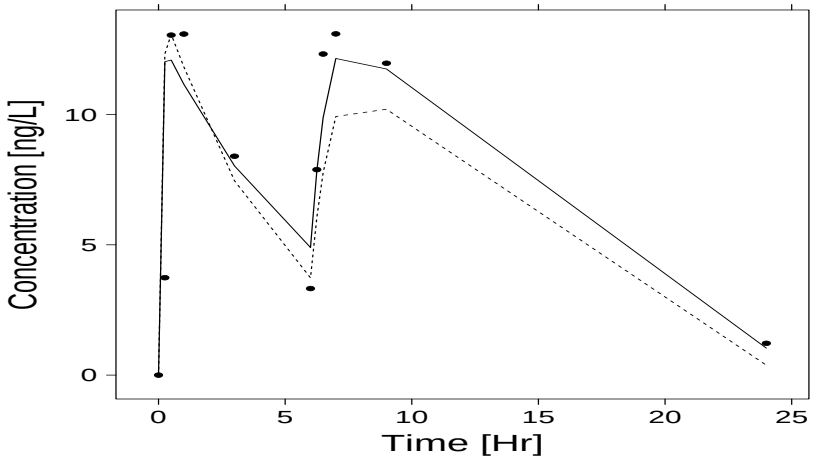

(b)

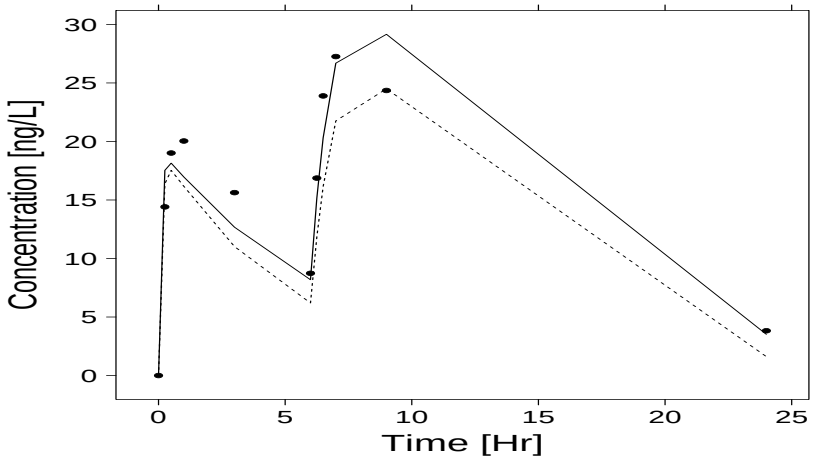

(c)

Figure 3.5: Obsereved concentrations (dots), population prediction (dashed line) and individual prediction (solid line) obtained from the PK analysis. Indivduals showed come from the three dosing groups: (a) 30 mg/kg/day, (b) 100 mg/kg/day and (c) 300 mg/kg/day.

	K_a		Cl		V
	FDD	SDD	M	F	
BSV (%)	8.0	86.8	4.2	5.9	4.7
CV (%)	28.2	28.2	69.7	69.7	49.7

Table 3.3: Estimates of the Between Subject Variability (expressed via percentage coefficient of variation) along with their precisions (expressed via percentage coefficient of variation) of the PK parameters.

	η_1	η_2	η_3
Sample Average	$1.24 \cdot 10^{-3}$	$-9.13 \cdot 10^{-3}$	$-1.37 \cdot 10^{-3}$
p-value	0.98	0.76	0.93

Table 3.4: Sample averages accross individuals of the random effects. The P-values come from a hypothesis test where the null hypothesis is that the mean of η_n is zero.

term of equation (2.3) was evaluated as $\sigma_1\%$, whilst the addittive term as σ_2.

	$Proportional(\epsilon_1)$	$Addittive(\epsilon_2)$
ISV	23.4%	0.144 ms
CV (%)	20.3	33.2

Table 3.5: Estimates of the Intra-Subject Variability (ISV) along with their precisions (expressed via percentage coefficient of variation) described in equation (2.3).

3.2 Pharmacodynamic Analysis

As it was already mentioned in section 1.4, the amount of information that Bayesian inference can provide is considerable and will be discussed in sections 3.2.2 and 3.2.3. Further, performing such analysis in WinBUGS entails the necessity of checking whether the different runs converged correctly (section 3.2.1).

3.2.1 MCMC Convergence Check

WinBUGS analysis is based on MCMC methods, a class of algorithms for sampling from probability distributions based on constructing a Markov chain that has the desired distribution as its equilibrium distribution (see [6] for details). An example of two Markov chains is shown in Figure 3.6, and a first step to assess the convergence is to visually check that the two chains are uncorrelated and overlap, which is the case for Figure 3.6.

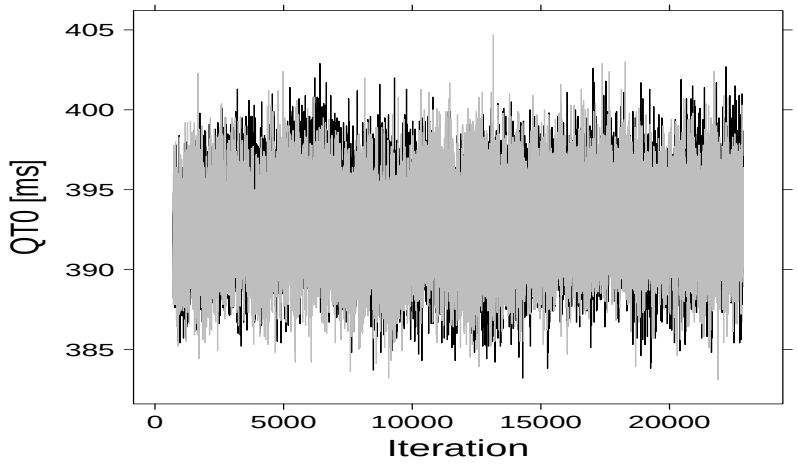

Figure 3.6: Standard output of a WinBUGS run: two Markov chains of QTc_0 parameter in humans.

A problem with MCMC methods is that convergence cannot always be diagnosed as clearly as in optimization methods. Indeed, there are several diagnostic tools that have been proposed since GIBBS sampling became popular in Bayesian inference ([16], [17], [18], [19]) and it may be very diffcult to satisfy all these criterions. In order to do not make the convergence check step too complex and lenghty, only the Gelman-Rubin diagnostic [17] will be performed, along with the assessment of low Monte Carlo (MC) errors, essential for precise estimation of the posterior distribution [20].
Gelman and Rubin method constits in different steps. Firstly, to evaluate the within chain variance W (hereafter $j = 1, ..., m$ chains, $i = 1, ..., n$ iterations and θ_{ij} is the i^{th} sample of the j^{th} chain of an arbitrary unknown parameter θ) as

$$W = \frac{1}{m} \sum_{j=1}^{m} s_j^2$$

where s_j^2 is the sample variance of θ in chain j:

$$s_j^2 = \frac{1}{n-1} \sum_{i=1}^{n} (\theta_{ij} - \bar{\theta}_j)^2$$

and $\bar{\theta}_j$ is the sample mean of θ in chain j:

$$\bar{\theta}_j = \frac{1}{n} \sum_{i=1}^{n} \theta_{ij}.$$

Secondly, to evaluate the between chain variance B as

$$B = \frac{n}{m-1} \sum_{j=1}^{m} \left(\bar{\theta}_j - \bar{\bar{\theta}} \right)^2$$

where $\bar{\bar{\theta}}$ is the sample mean θ between chains:

$$\bar{\bar{\theta}} = \frac{1}{m} \sum_{j=1}^{m} \bar{\theta}_j.$$

We can then estimate the variance of the stationary distribution as a weighted average of W and B, i.e.

$$\hat{\sigma}_\theta^2 = (1 - \frac{1}{n})W + \frac{1}{n}B,$$

that is used to define the final parameter of interest, named *Potential Scale Reduction Factor* (PRF)

$$PRF = \sqrt{\frac{\hat{\sigma}_\theta^2}{W}} \tag{3.1}$$

which should be as close to 1 as possible to state that the chains converged.

PRF values obtained from Markov chains of parameters of interest in both preclinical and clinical data are presented in Table 3.6. The same table contains also index ρ of equation (3.2), which helps to assess the convergence achievement in terms of MC error; particularly, ρ should be less than 5%.

$$\rho = \frac{MC_{error}}{SD_{estimate}} \cdot 100 \tag{3.2}$$

Table 3.6 suggests convergence of parameters A and ϕ in clinical data has not been totally achieved, as indicated by a $PRF > 1.5$ and a $\rho > 5\%$. Nevertheless, increasing the number of iterations does not solve the problem and the reason of a bad convergence most likely lays in the low amount of QT samples (8) collected from each patients trhougout the day. Moreover, in both species chains related to the drug effect parameter (i.e. *Slope*) also present convergence issues, and this might be due to the fact that the parameter is moslty zero (i.e. the drug effect is moslty absent) therefore chains struggle to overlap and follow a straight pattern since sample values range in a very limited interval (see Figure 3.7).

	PRF				
	QTc_0	α	A	ϕ	*Slope*
DOG	1.00	1.01	1.05	1.14	2.21
HUMAN	1.00	1.48	2.95	1.89	1.17
	$\boldsymbol{\rho}$ (%)				
DOG	0.92	0.98	1.29	2.65	6.11
HUMAN	1.49	4.76	5.57	5.17	5.69

Table 3.6: Potential Scale Reduction Factors and ρ indices obtained after running the WinBUGS model for both dog and human data.

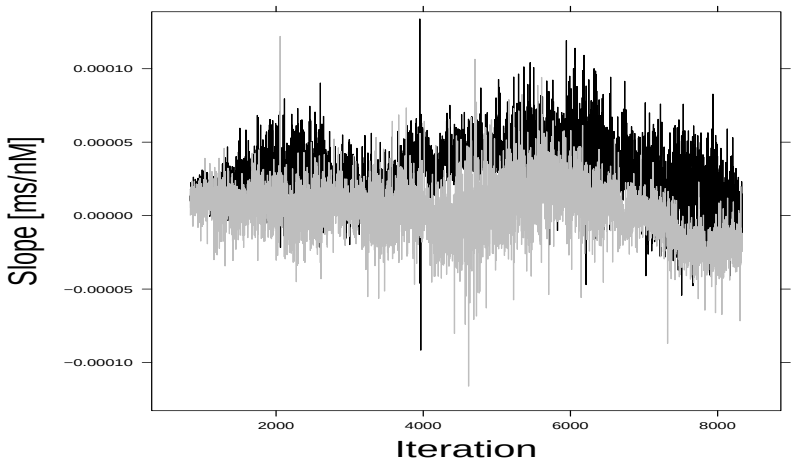

Figure 3.7: Markov chains of Slope parameter in preclinical data.

3.2.2 Preclinical Data

A thorough Bayesian analysis allows to estimate the full posterior distributions of the investigated parameters, enabling to extrapolate quantitative information by means of computing precentiles and means of such distributions. In regard to the PKPD model of equation (2.12), Figure 3.8 illustrates the probabilty density function (*pdf*) of parameters QTc_0, α, A, ϕ and *Slope* in conscious dog data. The shapes of these distributions supply a qualitative idea on the range of values assumed by the parameters. Also, the shape acts as an additional option of convergence inspection; the *pdf*, in fact, is an alternative way to represent the run Markov chains for that parameter, thereby it should not contain peaks and troughs since they would be evidence of lack of overlapping between chains as well as correlation within chain.

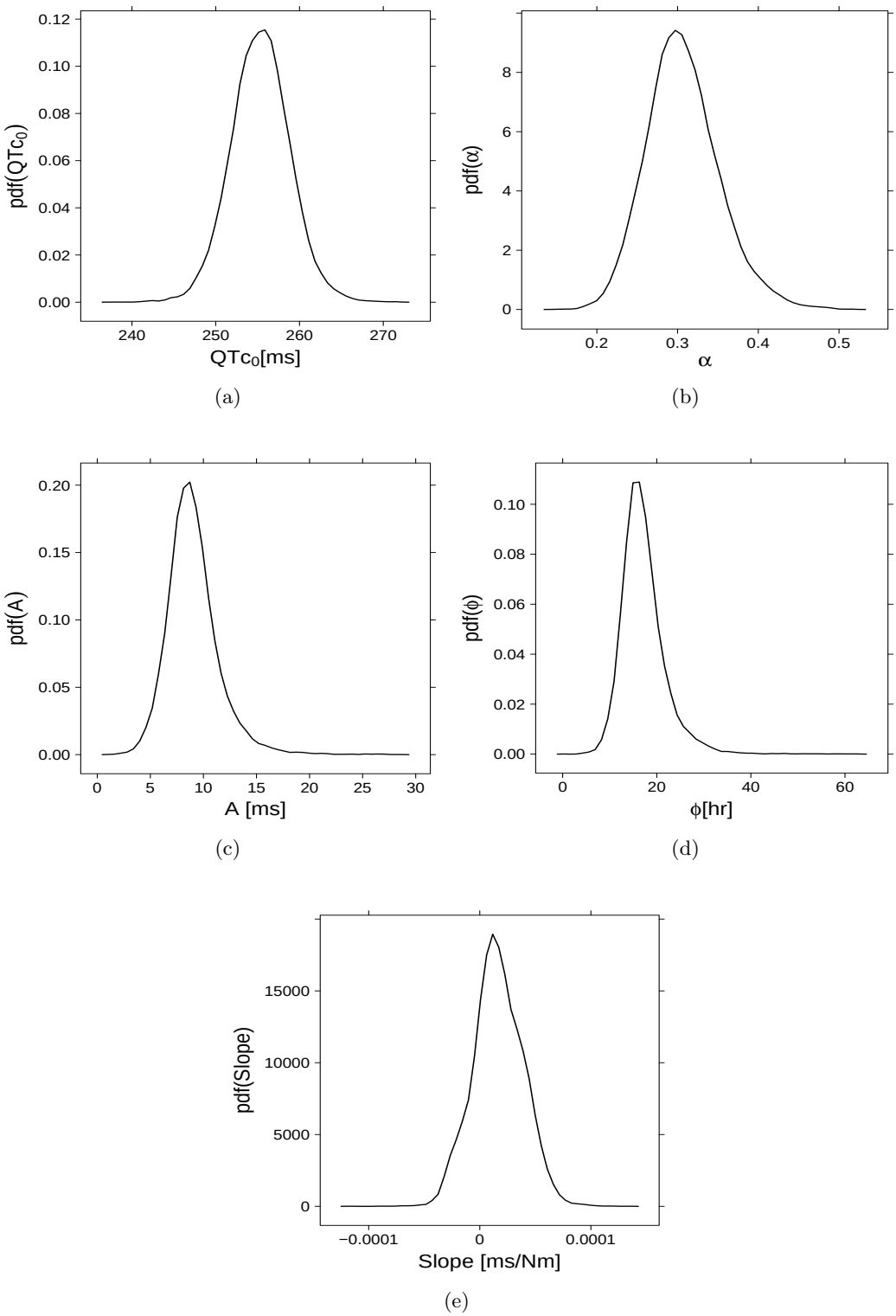

Figure 3.8: Posterior distributions of the PKPD model parameters in dog data: QTc_0 (a), α (b), A (c), ϕ (d) and *Slope* (e).

Posteriors obtained elucidates a successfull conclusion of the estimation step. Nonetheless, Figure 3.8e confirms what Table 3.6 had previoulsy told, i.e. a perfect convergence of *Slope* Markov chains is difficult to achieve as elicited from the irregular shape of the *pdf*.

	QTc_0 [ms]	α unitless	A [ms]	ϕ [hr]	*Slope* $[\frac{ms}{nM}]$
10% Credible Interval	251.0	0.251	6.34	12.24	$-1.2\cdot10^{-5}$
Mean	255.3	0.304	8.77	16.48	$1.6\cdot10^{-5}$
90% Credible Interval	259.7	0.365	11.93	22.68	$4.5\cdot10^{-5}$
CV (%)	1.4	14.9	28.1	28.2	136.6

Table 3.7: Mean, 80% credible intervals and precision (expressed as percentage coefficient of variation) of the population parameters of the PKPD model of equation (2.12) for dog data.

A statistical analysis on the posteriors leads to results in Table 3.7, where the parameter estimates are expressed in terms of posteriors' mean (i.e. the minimum mean square error (MMSE) estimator). Along with the MMSE estimator there are the 80% credible intervals and the precision of the estimates expressed as percent coefficient of variation.
Once again, the low precision on *Slope* estimate (136.6%) is an indicator of the problems arose in finding a complete convergence of the Markov chains for such parameter. An other interesting consideration that can be done by looking at Table 3.7 concerns the negative 10% credible interval of *Slope*, which stresses the fact that the drug effect lays around zero and therefore supports the conclusion that no drug induced QT prolongation takes place in dog.

	BSV					IOV	ISV
	QTc_0 %	α %	A %	ϕ %	*Slope** $\left[\frac{ms}{nM}\right]$	QTc_0 [ms]	σ_ϵ [ms]
10% Credible Interval	41.8	27.7	30.7	26.7	$2.0\cdot10^{-5}$	10.71	9.26
Mean	98.6	41.7	48.6	46.4	$3.8\cdot10^{-5}$	13.45	9.42
90% Credible Interval	403.1	74.8	96.0	91.2	$7.2\cdot10^{-5}$	17.50	9.59
CV (%)	166.6	153.2	229.1	177.1	164.9	43.0	1.4

*Because of *Slope* BSV 10% credible interval is negative, *Slope* BSV has not been represented via coefficient of variation since such measure is not definable for negative quantities.

Table 3.8: Mean, 80% credible intervals and precision (expressed as percentage coefficient of variation) of the random effects of the PKPD model of equation (2.12) for dog data.

Unlike standard ways of estimation, Basyesian estimation handles every enitity as a distribution, hence posteriors and credible intervals may be obtained also for parameters

conveying variability in the model, i.e. $\mathbf{\Omega}$ (Between Subject Variability), σ^2_λ (Inter Occasion Variability) and σ^2_ϵ (Intra Subject Variability). Table 3.8 contains MMSE estimator and 80% credible interval of parameters that quantify each source of variability. It may be noticed that CV values in BSV are all above 100%, reflecting an inaccurate estimate on how much the parameters vary amongst individuals. Such weakness in detecting reliable measures of the BSV is due to the very low number of dogs (4) enrolled in the PD study.

3.2.3 Clinical Data

Since there is no difference in the PKPD model between species, the same kind of dissection performed for preclinical data in section 3.2.2 will be presented. Starting from the estimated posterior distributions, Figure 3.9 shows profiles of A and ϕ are too wavy to conclude Markov chains for those parameters have fully convegred (Figure 3.9c and 3.9d), reinforcing the hypothesis made in section 3.2.1 that the number of QT measurements collected per day is too little to be able to extrapolate information on the cyrcadian rhythm.

	QTc_0 [ms]	α unitless	A [ms]	ϕ [hr]	$Slope$ $[\frac{ms}{nM}]$
10% Credible Interval	389.7	0.201	2.77	5.97	$1.6{\cdot}10^{-6}$
Mean	392.9	0.239	3.44	7.33	$4.2{\cdot}10^{-6}$
90% Credible Interval	396.1	0.275	4.09	8.59	$7.1{\cdot}10^{-6}$
CV (%)	0.6	12.2	23.0	27.1	52.9

Table 3.9: Mean, 80% credible intervals and precision (expressed as percentage coefficient of variation) of the population parameters of the PKPD model of equation (2.12) for clinical data.

	BSV					IOV	ISV
	QTc_0	α	A	ϕ	$Slope$	QTc_0	σ_ϵ
	%					[ms]	
10% Credible Interval	30.1	27.9	29.0	31.9	61.8	15.2	12.66
Mean	44.2	38.9	44.9	63.2	113.2	17.5	13.27
90% Credible Interval	81.5	58.1	69.2	104.4	292.0	20.3	13.94
CV (%)	47.7	29.4	35.0	45.6	37.8	23.2	3.8

Table 3.10: Mean, 80% credible intervals and precision (expressed as percentage coefficient of variation) of the random effects of the PKPD model of equation (2.12) for clinical data.

With regards to the MMSE estimates of the model's parameters, it has to be mentioned that results from human data lead to the same conclusions in terms of drug effect. Indeed,

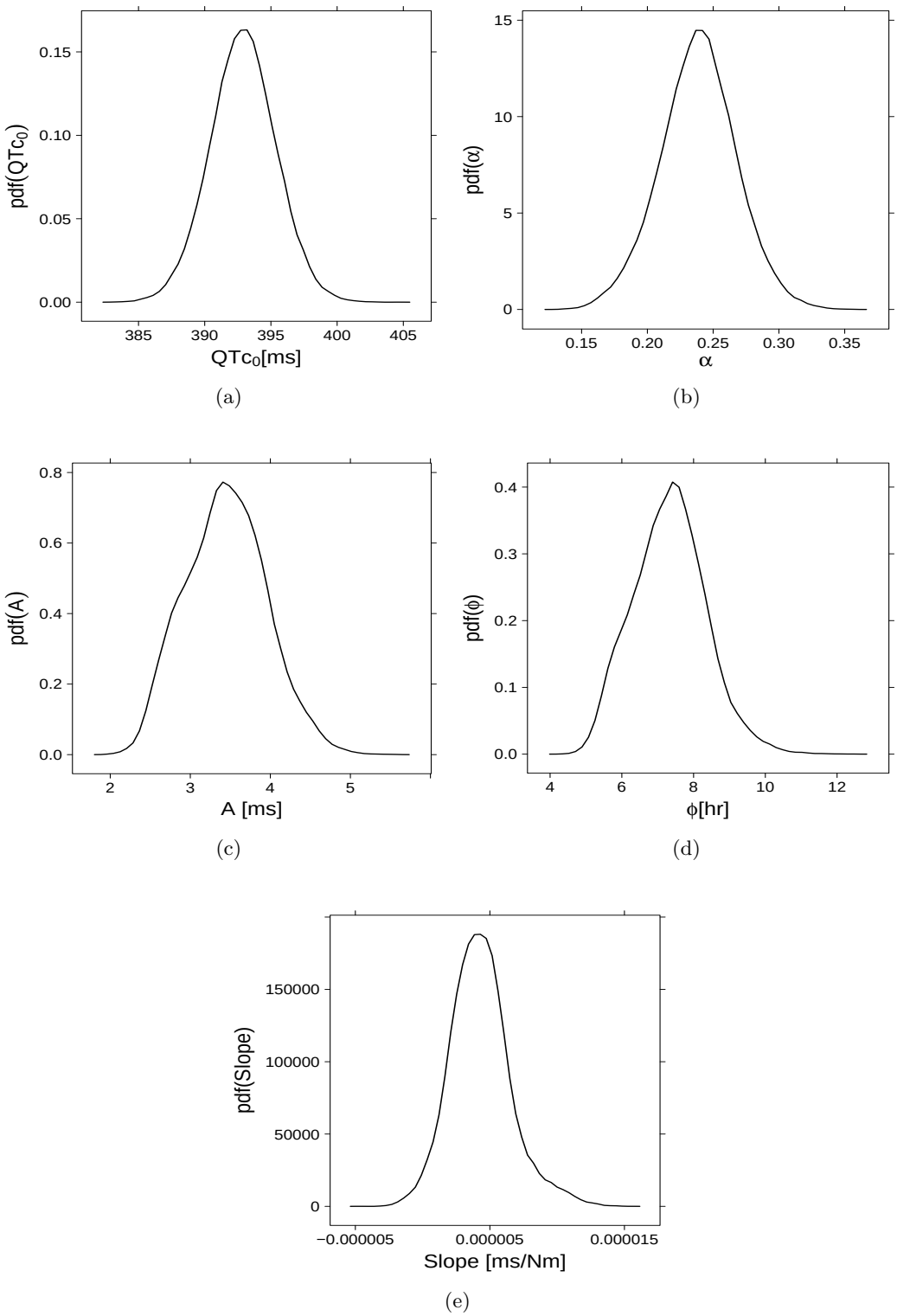

Figure 3.9: Posterior distributions of the PKPD model parameters in human data: QTc_0 (a), α (b), A (c), ϕ (d) and *Slope* (e).

as reported in Table 3.9, the *Slope* estimate is again (approximately) zero. Further, Table 3.10 confirms that with a reasonable number of individuals (45) estimates of BSV are sufficiently accurate (CVs are less than 50%). Nevertheless, because of the MMSE estimate of *Slope* is close to zero, the estimated BSV of this parameter is quite high; however, since it can be deduced the influence of drug effect in observed data is absent, there is no interest in the knolwedge of how *Slope* parameter varies among individuals.

Chapter 4

Conclusions

Concerning the assessment of risky QTc increases, according to regulatory guidelines [4] a threshold of 10 msec was used to explore the probability of QTc interval prolongation at the relevant therapeutic range. In particular, Table 4.1 enables to infer GSK945237 does not prolong QTc interval in either humans or dogs since the concentration needed to have a 50% probability of a QTc prolongation grater than 10 msec is approximately hundred times bigger than the predicted C_{max}.

	$PC_{50}^{\star}$ [nM]	C_{max} [nM]
DOG	3500000	62936.18
HUMAN	4200000	13096.86

*concentration associated with a P(QTc increase $\geq$ 10 msec) = 50%

Table 4.1: PC_{50} estimates and predicted C_{max} in both preclinical and clinical data.

These results differed from typically reported results in telemetered dogs, which are often based on non-parametric methods and statistical summaries of the data; yet, unlike traditional, data-driven experiments whose outcomes are often vague and ambigous, a model based approach provides a robust method to properly evaluate cardiovascular safety studies, allowing to advance clear and define conclusions. Moreover, the flexibility of the proposed approach, characterised by the usage of a Bayesian framework, eases and optimizes the interpretation of the results, as proven by the opportunity of obtaining the probability of a QTc prolongation greater than 10 msec (Figure 4.1). In fact, the assessment of a probability measure rather than a *yes or no* answer to the question: "is the QTc prolongation provoked by the drug under investigation matter of concern for further development of the molecule?" gives considerable advantages in a decision analysis context.

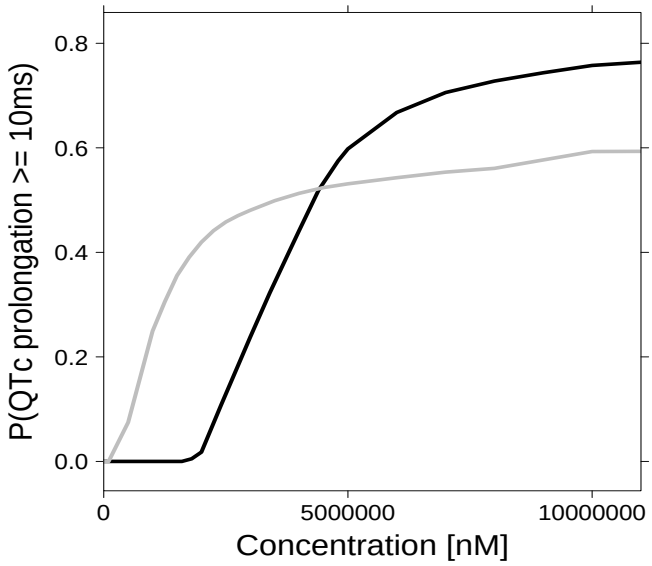

Figure 4.1: Curves showing the relationship between concentration and the probability of a QTc increase grater than 10 msec in dogs (gray line) and humans (black line).

Although no QTc-prolonging effects were observed, results illustrate the value of a quantitative approach to characterise drug effects in early drug development. Furthermore, the analysis reconfirms that accurate interpretation of pre-clinical findings requires suitable pharmacokinetic sampling and some understanding of expected therapeutic exposure.

In the context of translational pharmacology, the proposed model showed it is able to predict both human and dog data (see Figure 4.2) making its use suitable for interspecies scaling of QT interval prolongation. For this purpose, performing the presented analysis for an adeqaute number of compounds known to have QT prolonging effects may give essential information on the relationship of such drug effect between humans and dogs. In other words, estimation of *Slope* parameter in several drugs and in both species would allow to find the existing correlation of that parameter between human and dogs, bridging the gap between the two species and supporting decision making analysis at the very beginning of the development of a new compund.

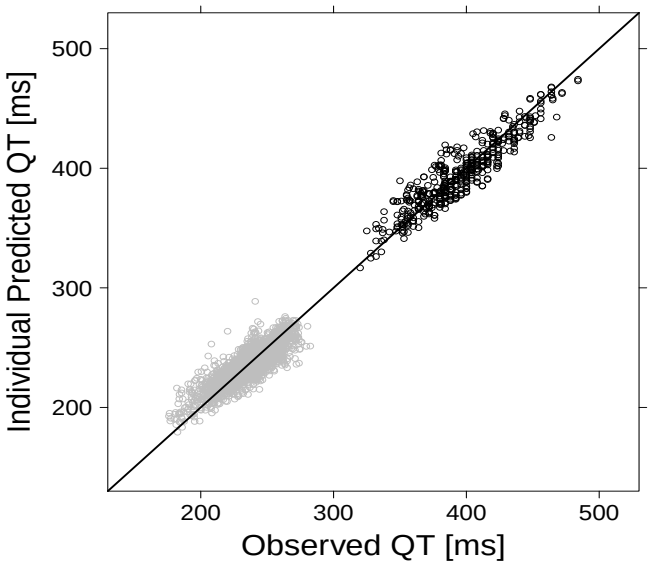

Figure 4.2: Individual goodness of fit plot of the PKPD model for both preclinical (gray dots) and clinical (black dots) data; the solid line represents the unity line. The model is capable to predict both dog and human QT interval.

Bibliography

[1] J. Milnes, O. Crociani, A. Arcangeli, J. Hancox, and H. Witchel, "Blockade of HERG Potassium Currents by Fluvoxamine: Incomplete Attenuation by S6 Mutations at F656 or Y652", *British Journal of Pharmacology*, vol. 139, pp. 887–898, 2003.

[2] J. Valentin, "Reducing QT Liability and Proarrhythmic Risk in Drug Discovery and Development", *British Journal of Pharmacology*, vol. 159, pp. 5–11, 2010.

[3] R. Fenichel, M. Malik, C. Antzelevitch, M. Sanguinetti, D. Roden, S. Priori, J. Ruskin, R. Lipicky, and L. Cantilena, "Drug-induced Torsades de Pointes and Implications for Drug Development", *Journal of Cardiovascular Elettrophysiology*, vol. 15, pp. 475–495, 2004.

[4] "Guidance for Industry: ICH E14 Clinical Evaluation of QT/QTc Interval Prolongation and Proarrythmic Potential for Non-Antiarrythmic Drugs", 2005. Department of Health and Human Services, Food and Drug Administration. http://www.fda.gov/downloads/RegulatoryInformation/Guidances/ucm129357.pdf.

[5] A. Chain, K. Krudys, M. Danhof, and O. Della Pasqua, "Assessing the Probability of Drug-Induced QTc-Interval Prolongation During Clinical Drug Development", *Clinical Pharmacology & Therapeutics*, 2011.

[6] D. Lunn, A. Thomas, N. Best, and D. Spiegelhalter, "WinBUGS – a Bayesian modelling framework: concepts, structure, and extensibility", *Cambridge, UK: MRC Biostatistic Unit*, vol. 10, pp. 325–337, 2000.

[7] S. Beal, L. Sheiner, A. Boeckmann, and R. Bauer, *NONMEM User's Guides (1989-2009)*. Icon Development Solutions, Ellicott City, MD, USA, 2009.

[8] J. Gabrielsson and D. Weiner, *PK/PD Data Analysis: Concepts and Applications*. Stockholm, Sweden: Swedish Pharmaceutical Press, 2007.

[9] H. Bazett, "An analysis of the time relations of electrocardiograms", *Heart*, vol. 7, pp. 353–370, 1920.

[10] L. Fridericia, "Die systolendauer im elektrokardiogramm bei normalen Menchen und bei Herzkranken", *Acta Med Scand*, vol. 53, pp. 469–486, 1920.

[11] W. Nelson, Y. Tong, J. Lee, and F. Halberg, "Methods for cosinorrhythmometry", *Chronobiologia*, vol. 6, pp. 305–323, 1979.

[12] Y. Touitou and E. Haus, *Biologic Rhythms in Clinical and Laboratory Medicine*. Berlin, Germany: Springer Verlag.

[13] K. Murphy, *Conjugate Bayesian Analysis of the Gaussian Distribution*, 2007. The Univeristy of Bristish Columbia. http://www.cs.ubc.ca/ murphyk/Papers/bayesGauss.pdf.

[14] "Jaws: repeated measures analysis of variance". WinBUGS Help Example on the Use of Wishart Distribution.

[15] M. O. Karlsson and N. Holford, "A tutorial on visual predictive check", 2008. Seventeenth PAGE meeting, Abstract 1434. www.page-meeting.org/?abstract=1434.

[16] J. Geweke, "Evaluating the accuracy of sampling-based approaches to calculating posterior moments", *Bayesian Statistics*, vol. 4, pp. 169–194, 1992.

[17] A. Gelman and D. Rubin, "Inference from iterative simulation using multiple sequences", *Statistical Science*, vol. 7, pp. 457–511, 1992.

[18] A. Raftery and S. Lewis, "How many iterations in the Gibbs sampler?", *Bayesian Statistics*, vol. 4, pp. 763–774, 1992.

[19] P. Heidelberger and P. Welch, "Simulation run length control in the presence of an initial transient", *Operations Research*, vol. 31, pp. 1109–1144, 1992.

[20] I. Ntzoufras, *Bayesian Modeling Using WinBUGS*. Hoboken, NJ, USA: John Wiley & Sons, Inc., 2008.